View Article Online
View Journal

Nanoscale Horizons

The home for rapid reports of exceptional significance in nanoscience and nanotechnology

Accepted Manuscript

This article can be cited before page numbers have been issued, to do this please use: A. K. Binder, F. Bremm, N. Feuchter, A. Torres-Coll, S. Kübel, C. Berking, S. Borrós, C. Fornaguera, N. Schaft and J. Dörrie, *Nanoscale Horiz.*, 2026, DOI: 10.1039/D5NH00667H.

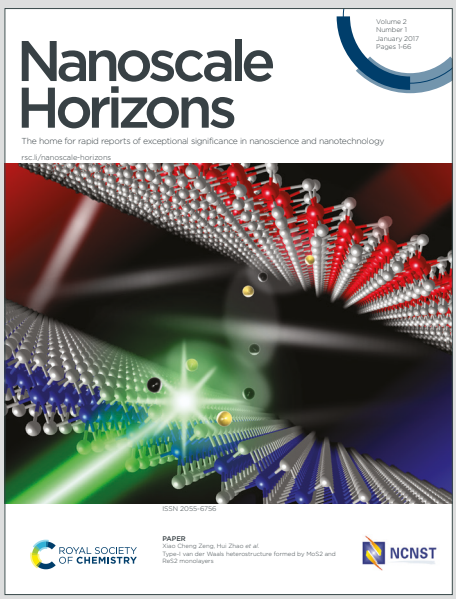

View Article Online
DOI: 10.1039/D5NH00667H

View Article Online
DOI: 10.1039/D5NH00667H

In this proof-of-concept-study, we show that CD80-mRNA transfected tumor cells can prime and expand human ex-vivo-isolated T cells, and that these cells gained the ability to lyse the tumor cells. Importantly, the T cells primed with the CD80-expressing tumor cells were also capable of lysing untransfected tumor cells with similar efficiency. While the original idea dates back two decades, it has never been exploited with human material, and the use of the newly developed poly(β-amino ester) nanoparticles allows clinical implementation. In addition, the concerns about a possible stimulation of the immune checkpoint receptor CTLA-4 on the T cells, which represent an unwanted but natural alternative receptor for CD80 was addressed and appeased, since CTLA-4 expression was indeed reduced by stimulation with the CD80-expressing tumor cells. In sharp contrast, the CD80-untransfected tumor cells induced the expression of this and other checkpoint receptors. Hence, our study shows that a nanoscience-based approach is suitable to implement a new tumor treatment strategy involving nanoparticle-encapsulated mRNA.

View Article Online
DOI: 10.1039/D5NH00667H

ARTICLE

Received 00th January 20xx,
Accepted 00th January 20xx

DOI: 10.1039/x0xx00000x

Transforming Tumor Cells into Professional Antigen-Presenting Cells Using Poly(β-amino Ester) Nanoparticles to Deliver CD80-encoding mRNA

Amanda Katharina Binder[a,b,c,d], Franziska Bremm[a,b,c,d], Niklas Feuchter[a,b,c,d], Antoni Torres-Coll[e], Sabrina Kübel[f], Carola Berking[a,b,c,d], Salvador Borrós[e], Cristina Fornaguera[e], Niels Schaft[a,b,c,d†], Jan Dörrie[a,b,c,d†*]

Effective T-cell activation requires both antigen recognition and co-stimulatory signaling. However, tumor cells typically lack the necessary co-stimulatory molecules, rendering T-cell receptor engagement with tumor antigens insufficient to induce potent anti-tumor immune responses. To overcome this limitation, we converted tumor cells into professional antigen-presenting cell (APC)-like cells by equipping them with the co-stimulatory molecule CD80. Electroporation of melanoma and lung cancer cell lines with CD80-encoding mRNA significantly increased their ability to stimulate tumor-antigen-specific T cells, as indicated by increased activation markers and cytokine secretion. Most importantly, CD80 expression converted melanoma cells into APC-like cells capable of priming and expanding naïve T cells that recognize endogenous tumor antigens. To enable clinical application, we subsequently used poly-(beta aminoester) (pBAE) polymers, which efficiently encapsulate mRNA into nanometric polyplexes. As previously reported, pBAE nanoparticles (NPs) efficiently penetrate plasma membranes and escape endosomal degradation both *in vitro* and *in vivo*. Here, we evaluated pBAE NPs encapsulating GFP-encoding mRNA in human cell lines derived from melanoma, lung cancer, leukemia, adenocarcinoma, uveal melanoma, and Merkel cell carcinoma. The pBAE NPs effectively transfected adherent tumor cells, and tumor spheroids *in vitro* and *in ovo*. When delivering CD80 mRNA, NPs achieved expression rates of more than 50% in most cell lines, which lasted for at least 72 h. Here as well, nanoparticle-mediated CD80 expression enabled melanoma cells to prime and expand naïve T cells recognizing endogenous tumor antigens. Importantly, T cells primed by CD80-expressing tumor cells were also capable of killing tumor cells that had not been transfected. In line with these findings, T cells stimulated with untransfected tumor cells showed high levels of checkpoint receptors CTLA-4 and PD-1, whereas the expression was significantly lower when using CD80-transfected tumor cells. This proof-of-concept study indicates that conversion of tumor cells into professional APC-like cells with CD80 mRNA is feasible and results in potent anti-tumor $CD8^+$ T-cell responses. With the use of mRNA-loaded pBAEs, the prerequisites for a future application *in vivo* are given. Therefore, the application of pBAE NPs encapsulating CD80 mRNA to specifically transfect tumor cells presents a new promising strategy for the *in vivo* treatment of various cancers.

[a]*Department of Dermatology, Friedrich-Alexander-Universität Erlangen-Nürnberg, Uniklinikum Erlangen, Erlangen, Germany*
[b]*Comprehensive Cancer Center Erlangen - European Metropolitan Area of Nuremberg (CCC ER-EMN), Erlangen, Germany*
[c]*Deutsches Zentrum Immuntherapie (DZI), Erlangen, Germany*
[d]*Bavarian Cancer Research Center (BZKF), Erlangen, Germany*
[e]*Grup d'Enginyeria de Materials (Gemat), Institut Químic de Sarrià (IQS), Universitat Ramon Llull (URL), Barcelona, Spain*
[f]*Institute of Clinical and Molecular Virology, Universitätsklinikum Erlangen, Friedrich-Alexander-Universität Erlangen-Nürnberg, Erlangen, Germany*
†*These authors share senior authorship*
**Correspondence: Jan Dörrie (jan.doerrie@uk-erlangen.de)*
Supplementary Information available: [details of any supplementary information available should be included here]. See DOI: 10.1039/x0xx00000x

Introduction

Insufficient activation of cytotoxic T cells is considered a major factor underlying ineffective anti-tumor immune responses. Although tumor cells express tumor-associated antigens, they are generally poor inducers of antigen-specific T-cell responses and lack the capacity to prime naïve T cells. Moreover, tumors establish an immunosuppressive microenvironment that actively limits anti-tumor immunity. Within this environment, inhibitory molecules not only impair cytotoxic T-cell effector functions but also suppress the activity of professional antigen-

View Article Online
DOI: 10.1039/D5NH00667H

presenting cells (APCs), thereby further reducing effective T-cell activation (1-7). This results in impaired tumor cell recognition, antigen presentation, and cytotoxic T-cell activation, thus leading to tumor cell growth and metastasis formation (8, 9). Consequently, restoring the priming of cytotoxic T cells within the tumor microenvironment can be a promising strategy in the development of anti-tumoral immunotherapies.

Effective T-cell priming is typically restricted to professional APCs, which provide both essential signals required for activation: recognition of antigens presented on MHC complexes and a co-stimulatory signal. One important co-stimulatory molecule is CD80 (B7-1), a transmembrane glycoprotein and a member of the B7 family as well as the Ig superfamily (10). CD80 is primarily expressed on professional APCs, such as dendritic cells and macrophages, and provides the essential co-stimulatory signal for full T-cell activation in addition to the antigen presented on MHC complexes (11). Both signals are delivered in close spatial proximity within the immunological synapse formed between APC and the T cell (12). The respective stimulatory receptor for CD80, which is primarily expressed on naïve and memory T cells is CD28. Both T cell types require a CD28-activating co-stimulatory signal to function effectively (13). In addition, activated T cells express the inhibitory receptor CTLA-4 (cytotoxic T lymphocyte-associated protein 4), which induces opposite effects on T cells in a negative feedback loop (14, 15).

Upon MHC:TCR engagement, the CD80:CD28 interaction promotes T-cell activation accompanied by a broad transcriptional change in the T cells (14). Intracellular signaling pathways of CD28 activation induce, among others, the nuclear factor-κB (NF-κB), activator protein 1 (AP-1), and nuclear factor of activated T cells (NFAT) (16-18). Following transcriptional changes include the expression of the anti-apoptotic protein B-cell lymphoma-extra large (Bcl-XL) and enhanced T-cell effector cytokine expression especially of IL-2 (19-21). Thus, T-cell survival is maintained as well as proliferation and activation are induced. The absence of CD80:CD28 interaction in the presence of MHC:TCR recognition leads to clonal anergy of T cells (22, 23). Due to the importance of CD80 in the process of activating T cell efficiently, multiple studies have investigated the potential use of CD80 in an immunotherapeutic strategy. In a pioneering *in vitro* experiment, Kaufmann et al. transfected human cervical cancer cell lines with a CD80 expression plasmid and showed their increased ability to stimulate allogenic $CD4^+$ and $CD8^+$ T cells, which were in turn able to lyse parental tumor cells (24). Already in the same year, CD80-expressing tumor cells were used successfully as a therapeutic vaccination in early stages of an acute myelogenous leukemia mouse model (25). The induced anti-tumor immunity was long-lasting and was depended on $CD8^+$ T-cell activation.

The clinical studies that exploited the immunostimulatory effect of CD80 generally consisted of allogenic tumor cells, which were genetically modified to express CD80. In breast cancer, this was applied in two phase I clinical trials, NCT01127074 (26) and NCT00003184, the latter with a minority of patients showing an immune response (27). Another phase I/II clinical trial (NCT01265368) tested a cancer cell vaccine (MGN1601) consisting of genetically modified allogenic tumor cells expressing IL-7, GM-CSF, CD80, and CD154 in advanced renal cell carcinoma patients. Here, one patient showed remission, and seven patients developed a stable disease (28, 29). In summary, artificially induced high CD80 expression of tumor cells showed therapeutic potential. Nevertheless, the antigen repertoire of the allogenic tumor cells might not match with the patient's tumor cells, which induces a misguided T-cell response and albeit being allogenic, the injection of living tumor cells brings additional safety concerns. To avoid these risks and the high costs of the generation of such cellular therapeutics, recent developments in mRNA technology could represent an innovative treatment strategy to deliver CD80-encoding mRNA specifically to the tumor cells in situ.

Cancer treatment strategies based on mRNA have several advantages. Treated patients usually experience tolerable adverse events and low toxicity due to the fast and easy degradation of the mRNA (30). The mRNA can encode for tumor antigens, cytokines, tumor suppressors, Cas9 for genome editing, chimeric antigen receptors, and T-cell receptors while excluding an irreversible genome integration (30, 31). Originally, such vaccines had to be administered as naked mRNA, which faces the problem of too fast degradation (32, 33), or the mRNA was to be delivered as cellular vaccine within dendritic cells, which were transfected ex vivo. Recent developments have created new delivery methods by conjugating the nucleic acid with protamine or encapsulating the mRNA in biodegradable lipoplexes and lipid nanoparticles (NPs) (34). These have shown high capabilities in inducing efficient and profound anti-tumor immune responses, with some of them already tested in clinical trials (31, 35-40). However, all these formulations included a component modified with poly(ethylene glycol) (PEG). Although traditionally referred to as safe, lately, some studies reporting the generation of anti-PEG antibodies as a rejection response in repeated administration therapies have aroused controversy on the use of PEG-derived products (41). Additionally, neither of these lipid-based nanoformulations contains a targeting moiety, fact very difficult due to the limited availability of lipid macromolecules required for the formation of the nanoparticles. In this context, we developed some years ago alternative polymeric carriers, based on poly-(beta aminoester) (pBAE) biocompatible and biodegradable polymers. Adding cationic peptides at their end-terminus, we demonstrated the capacity of pBAE polymers to electrostatically complex mRNA, forming small nanometric particles (42-44). We demonstrated their superior capacity to penetrate plasmatic cell membranes and boost endosomal escape, thus resulting in high transfection efficacies *in vitro* and *in vivo*, namely for tumor cells. Being these polymers synthesized from a bottom up strategy, extensive libraries of pBAE variants exist, making it possible to modulate properties such as hydrophobicity, MW and targeting moieties inclusion. Additionally, PEG is not a must for the functioning of the polymer. We also demonstrated their use for immune modulatory applications in oncology, among others (45, 46).

Therefore, mRNA-based cancer therapeutics, composed of pBAE NPs, offer a new approach to an off-the-shelf therapeutic

agent for the delivery of CD80-encoding mRNA into tumor cells of patients in situ where T cells can be efficiently and specifically activated.

Here we investigate the effect of CD80 expression on different tumor cell lines on their ability to stimulate tumor antigen-specific T cells and to prime and expand naïve human $CD8^+$ T cells. We then examine the ability of mRNA encapsulated in pBAE NPs to transfect the various tumor cell lines. Finally, we showed that pBAE NP-based transfection of tumor cells with CD80 also resulted in their ability to prime and expand naïve human $CD8^+$ T cells against the endogenously expressed melanoma antigen MelanA.

Material and Methods

Materials

The supplements for cell culture media were purchased from Lonza (Verviers, Belgium; RPMI1640, L-glutamine. Gentamycin, sodium pyruvate, MEM nonessential aa), Merck KGaA (Darmstadt, Germany; fetal bovine serum/FBS), PAA Labortechnik and GE Healthcare Life Sciences (Pasching/Linz, Austria; HEPES), Gibco (USA; beta-mercaptoethanol), Sigma-Aldrich (St. Louis, MO, USA; human AB serum). EDTA was purchased from Lonza (Verviers, Belgium) and the cytokines IL-2 and IL-7 were used from Miltenyi (Bergisch Gladbach, Germany). For $CD8^+$ T-cell isolation, Lymphoprep from Axis-Shield PoC AS (Oslo, Norway) and CD8 MACS beads from Miltenyi (Bergisch Gladbach, Germany) were used.

mRNA encoding CD80 and the TCRs was generated using the *in-vitro* transcription kit with T7 RNA polymerase (mMESSAGE mMACHINE kit; Ambion, ThermoFisher Scientific, Darmstadt, Germany), according to the manufacturer's instructions. Opti-MEM™ was purchased from Gibco (USA). Reagents and solvents used for synthesis were purchased from Sigma Aldrich and Panreac and used as received unless otherwise stated. CK3 (NH2-Cys-Lys-Lys-Lys-COOH) and CH3 (NH2-Cys-His-His-His-COOH) peptides was obtained from GL Biochem (Shangai) Ltd with a purity of at least 98%. MelanA and MAGE-A3 peptides were obtained from GenScript Biotech (Rijswijk, Netherlands). HLA-A*02:01-PE ELAGIGILTV tetramer was synthesized by Biozol (Hamburg, Germany), and the dextramer by Immudex (Virum, Denmark).

The antibodies used in FACS, anti-CD27-APC, anti-CD45RA-BV421, anti-CD8-PE-Cy7, anti-CCR7-FITC, anti-CD25-BV421, anti-CD3-APC-H7, anti-CTLA-4-APC, anti-PD-1-PE, and anti-CD80-PE were all purchased from BD Bioscience (Heidelberg, Germany). The anti-CD69-APC was from BioLegend (San Diego, USA). The Th1/Th2 Cytometric Bead Array Kit was from BD Bioscience (Heidelberg, Germany).

Cell culture

The following cell lines were used: The Merkel Cell Carcinoma cell lines WaGa (Houben et al., 2010), MKL-1 (Rosen et al., 1987), and MKL-2 (Martin et al., 1991) were kindly provided by Jürgen Becker (DKTK, Essen, Germany); The cutaneous melanoma cell lines Mel526 was kindly provided by Hinrich Abken (Leibnitz Institute, Regensburg, Germany) and A375M (47) was kindly provided by Corlien Aarnoudse (Universiteit Leiden, The Netherlands); The uveal melanoma cell lines Mel270 and OMM2.5 were kindly provided by Martine Jager (University of Leiden, The Netherlands); The acute monocytic leukemia cell line THP1 was kindly provided by Markus Biburger (Erlangen, Germany); The lung cancer cell lines PC9, H1975, A549, and 11-18 were kindly provided by Rafael Rosell (University Hospital Sagrat Cor, Barcelona, Spain) .

All cell lines were cultured in R10 medium consisting of RPMI1640 supplemented with 10% FBS, 2 mM L-glutamine, gentamycin (20 mg/L), 10 mM HEPES, and 20 mM beta-mercaptoethanol. All cell lines were kept at 37°C in 5% CO2, and split according to their density. Adherent cell lines were detached with PBS-EDTA. All cell lines were regularly tested for mycoplasma.

Generation of T cells from whole human blood

The blood of healthy donors was obtained following informed consent and approval of the institutional review board (ethics committee of the Friedrich-Alexander-Universität Erlangen-Nürnberg, Erlangen, Germany: Ref. no. 4158). After mononuclear cells were isolated using density centrifugation with Lymphoprep, CD8 MACS beads were used to isolate the $CD8^+$ T cells. For TCR-transfection, T cells were rested overnight in T-cell medium consisting of RPMI 1640, 10% human AB serum, 2 mM L-glutamine, 20 mg/L gentamycin, 10 mM HEPES, 1 mM sodium pyruvate, and 1% MEM nonessential aa, supplemented with 1000 U/mL IL-7 at a concentration of 2-3x10^6 cells/mL. For MelanA-specific priming, the $CD8^+$ T cells were used immediately after MACS.

mRNA electroporation of tumor cells and T cells

mRNA encoding CD80 and TCRs were generated using the *in-vitro* transcription kit with T7 RNA polymerase according to the manufacturer's instructions. Template plasmids were generated as described previously (48). The transfection with RNA was performed as described by Sauerer *et al.* (49). Cells were harvested and washed in Opti-MEM™. The maximum concentration for electroporation of tumor cells was 6x10^7 cells/mL Opti-MEM™ and of isolated T-cells it was 12 x10^7 cells/mL Opti-MEM™. Depending on size, the cells were electroporated between 1 and 5 ms (square-wave pulse, 1250 V/cm) and rapidly transferred to their respective medium. T cells were electroporated with 15 µg of each the alpha and beta chains of the respective T-cell receptors gp100 (50), MAGE-A3, and MelanA (48). Fifteen µg of CD80 RNA or 5 µg of GFP RNA were used to electroporate the tumor cells.

Transfection of tumor cells via nanoparticles

Poly(β-amino ester)s (pBAEs) were synthesized as described in Dosta *et al.* (51). Briefly, addition reaction of primary amines to an excess of diacrylates was used to synthesize an acrylate-terminated polymer. Then, this polymer was end-capped with oligopeptide composed of Cys + 3 Lys (CKKK or CK3) or Cys + 3His (CHHH or CH3), in DMSO, obtaining the K or H polymer

View Article Online DOI: 10.1039/D5NH00667H

respectively. Synthesized structures were confirmed by 1H NMR, recorded in a 400 MHz Varian (NMR Instruments, Claredon Hills, IL) and methanol-d4 used as a solvent. Molecular weight (MW) relative to polystyrene standard was determined by HPLC (HPLC Elite LaChrom system of VWR-Hitech equipped with a GPC Shodex KF-603 column and THF as mobile phase).

To formulate the NPs, K and H polymers were mixed in a ratio of 60:40 in sterile filtered 12.5 mM sodium acetate buffer. To generate fluorescent NPs, H polymers were spiked with 10% Cy5-tagged H polymers. The mRNA was diluted in sterile filtered 12.5 mM sodium acetate buffer. For the NP formation, the mRNA was added to the polymer mix by vigorous pipetting. Then the formulation rested for 10 min at RT. Afterwards, the volume was doubled by adding ddH_2O and the solution was stored at 4°C until use, never longer than 6 hours. The quality of each batch of NPs was confirmed using a Zetasizer Advance Pro (Malvern Panalytical). Therefore, 10 µL of the NP suspension were added into 990 µL ddH_2O and given into a 10°mm polystyrene cuvette. The characteristics of the NPs were determined by three repetitions of 14 single measurements with sterile water at 25°C. The NPs were defined as good and useable for experiments when their Z-average (intensity-weighted mean hydrodynamic size) was between 100 and 160 and had a size distribution measured by the polydispersity index (PdI) below 0.2. NPs were applied in concentrations that delivered 0.625 µg mRNA (5 µL NP solution) per well in 96-well plates and 1.25 µg (10 µL NP solution) in 24-well plates. The transfection was conducted in the presence of full supplemented media for at least 16 hours. For visualization of transfection, Cy5-tagged NPs were used, and cells were transfected on a cellstar µclear black 96 well plate (Greiner Bio-one, Frickenhausen, Germany) using 2.5 µL NP solution, and imaged using an ImageXpress Pico (Molecular Devices, San Jose, CA, USA). Image analysis and processing were performed using ImageJ.

Transfection of tumor spheroids and CAM assay

For imaging of tumor spheroids, 2,000 Mel526 cells were seeded into ultra-low attachment Nunclon™ Sphera™ 96-well U-bottom plates (Thermo Fisher Scientific) and cultured for 7 days to allow spheroid formation. Spheroids were transfected with 5 µL NP solution and imaged using an AMG microscope 24 h post-transfection.

For time-course analysis of transfection efficiency, 10,000 Mel526 cells were seeded into ultra-low attachment Nunclon™ Sphera™ 96-well U-bottom plates and cultured for 14 days to allow organically spheroid formation and generate sufficient numbers for flow cytometric analysis. The culture medium was replaced regularly. On day 14, 5 µL of GFP mRNA or CD80 mRNA NP solution was added to each well. After 24, 48, or 72 h of incubation, spheroids were washed with PBS and dissociated using PBS-EDTA for 20 min at 37 °C. Single-cell suspensions were generated by gentle pipetting for subsequent analysis.

The chorioallantoic membrane (CAM) assay was performed as generally described before (52). Briefly, fertilized chicken eggs (Lohmann, Ankum, Germany) were incubated in a humidified egg incubator (Wiltec Wildanger Technik GmbH, Eschweiler, Germany) at 37 °C temperature and approximately 55 % humidity until embryonic development day (EDD) 3. On EDD3, a window was cut into the eggshell and resealed with adhesive tape to monitor successful fertilization.

For tumor transplantation, Mel526 spheroids were generated *in vitro* by seeding 250,000 cells into ultra-low attachment Nunclon™ Sphera™ 96-well U-bottom plates and culturing them for 48 h with regular medium changes. On EDD8, a silicone ring was placed onto the CAM, and one tumor spheroid was transferred into the ring in 70 µL R10 medium. The window was resealed, and eggs were further incubated until EDD14.

On EDD13, freshly prepared GFP mRNA nanoparticles were administered by pipetting 40 µL of NP solution directly into the silicone ring containing the tumor spheroid. After 32 h of incubation, the tumor-bearing CAM area including the silicone ring was excised and analyzed immediately using the fluorescence microscope EVOS AMG (Advanced microscopy group INC, Mill Creek, USA). Embryos were decapitated and discarded to terminate the experiment on day 14 of embryo development. According to EU jurisdiction, experiments on chicken embryos terminated until day 18 of development are not considered animal experiments and need not to be declared (52).

Co-culture of TCR-transfected $CD8^+$ T cells and tumor cells

Tumor cells were harvested and either transfected with CD80 RNA via NPs or electroporation and left to rest overnight. Then, the tumor cells were washed and loaded with 10 µg/mL peptide in R10 medium for 1 h at 37°C in 5% CO_2. Peptide sequences were: EAAGIGILTV for MelanA, YLEPGPVTA for gp100, and EVDPIGHLY for MAGE-A3. Unbound peptides were washed off and fresh R10 medium was added to the cells. Having isolated the $CD8^+$ T cells via MACS beads the day before, the T cells were electroporated with the indicated TCRs and incubated with the respective tumor cells (100,000 tumor cells: 100,000 T cells) in 200 µl in a 96-well plate overnight. Then T cells were harvested and analyzed for expression of CD25 and CD69 by flow cytometry and cytokine concentrations in the supernatants were measured using a Th1/Th2 cytometric bead array kit following the manufacturer's instructions (BD Bioscience).

Flow cytometry readout for the CD80, GFP expression, and T-cell activation

The cells from the co-culture of $CD8^+$ T cells and tumor cells were harvested, washed in FACS buffer, and incubated for 30 min at 4 °C with anti-CD80-PE, anti-CD3-APC-H7, anti-CD25-BV421, and anti-CD69-APC. Intrinsic expression of GFP was measured without additional staining. Then all washed and re-suspended cells were analyzed with a FACSCanto II flow cytometer and FlowJo10 software. The gating strategy for activated T cells and tumor cells is provided in the supplements (**Fig. S1** and **S2**).

Priming of MelanA-specific $CD8^+$ T cells by electroporated tumor cells

View Article Online
DOI: 10.1039/D5NH00667H

Mel526 cells were CD80 electroporated one day before the cell culture (d0) and rested for 24 h in their respective medium at 37°C, 95% humidity and 5% CO_2. On d1, $CD80^+$ Mel526 and non-electroporated Mel526 were harvested, counted and seeded with 100.000 cells per well in a 24-well plate. The tumor cells rested for 2-3 hours and then loaded with MelanA peptide. At the same day, $CD8^+$ T cells were isolated from human whole blood of HLA-A*02:01 donors. Directly after the MACS isolation, 10^6 $CD8^+$ T cells were given into to the prepared wells with tumor cells and respective control wells, each with a total volume of 2 mL. On day 2 and day 4, IL-2 and IL-7 were added to wells with T cells. The media was exchanged every other day by carefully discarding 1.5 mL supernatant and adding 1.5 mL fresh media. On day 6, fresh Mel526 cells were prepared for re-stimulation. The Mel526 cells were electroporated with CD80 and rested for 24 h in their respective medium at 37°C, 95% humidity and 5% CO_2. On day 7, the CD80-transfected Mel526 cells and non-electroporated Mel526 cells were harvested, counted and seeded with 10^5 cells per well in a 24-well plate. After resting for 2-3 hours, the tumor cells were loaded with MelanA peptide. Afterwards IL-2 and IL-7 were added to the wells. The medium was exchanged every day by carefully discarding 1.5 mL supernatant and adding 1.5mL fresh media. If needed, the wells were split on day 9. On day 14 the stimulation was terminated and flow cytometry analysis was conducted.

Priming of MelanA-specific $CD8^+$ T cells by nanoparticle transfected tumor cells

One day before co-culture (day 0), Mel526 cells were harvested, counted and seeded with 10^5 cells per well in 1 mL of their respective medium. Cells rested for 5 hours at 37°C, 95% humidity and 5% CO_2. CD80 and GFP NPs were freshly prepared and directly added into the wells, afterwards carefully mixed with the medium by pipetting. As controls served untreated Mel526 cells and T cells only. The transfection was conducted over night, at least for 16 hours. On day 1, $CD8^+$ T cells were isolated from human whole blood of HLA-A*02:01 donors. Shortly before the addition of the T cells to the tumor cells, the medium was exchanged. The T cells were added directly after the MACS isolation, 10^6 $CD8^+$ T cells were given into to the prepared wells with tumor cells and respective control wells each with a total volume of 2 mL. The co-culture was stored at 37°C, 95% humidity and 5% CO_2. On day 2, day 4, day 7, and day 9, IL-2 and IL-7 were added to wells with T cells. The media was exchanged every other day by carefully discarding 1.5 mL supernatant and adding 1.5 mL fresh media. As restimulation, the CD80 or GFP NPs were added at day 6, day 8, and day 10. If needed, the wells were split on day 7. On day 14 the stimulation was terminated and flow cytometry analysis was conducted.

HLA multimer and immune checkpoint staining of primed $CD8^+$ T cells

The primed and re-stimulated $CD8^+$ T cells were harvested and T cells specific for the MelanA peptide were detected by incubation with HLA-A*02:01-PE ELAGIGILTV tetramer or dextramer for 30 min at room temperature. Afterwards, anti-CD27-APC, anti-CD45RA-BV421, anti-CD8-PE-Cy7, anti-CCR7-FITC, anti-CTLA-4-APC, and anti-PD-1-PE were added directly and incubated for another 30 min at 4°C. The cells were washed and analyzed with a FACSCanto II flow cytometer and the FlowJo10 software. The gating strategy for identification of MelanA-specific T cells can be found in the supplements (**Fig. S4**).

Cytotoxic potential of primed $CD8^+$ T cells against tumor cells

Mel526 cells were electroporated with CD80 mRNA or without RNA and used as target cells on the next day in a chromium release assay. Tumor cells were labelled with 20 µl ^{51}Cr at 1 mCi/200 µl in per 100 µl 20 % FCS (1 µCi Na2 $51CrO_4$/µl of cells) for one hour and co-cultured with primed $CD8^+$ T cells in R10 at ratios of target to effector cells of 1:60, 1:20, 1:6, and 1:2. Tumor cells without T cells were used to determine the background release whereas the lysis of target cells by 0.5% Nonidet P40 was used as maximum release. After 4 hours at 37°C, supernatant of the co-culture was mixed with scintillation fluid and analyzed for the released radioactivity with the PerkinEkmer 2450 MicroBeta Scintillation Counter. Raw counts were normalized to the percentage of cytolysis with the following formula: [(measured release - background release)] / [(maximum release - background release)] x 100 %.

Statistics

Statistical analysis and data visualization were performed using GraphPad Prism software, version 10.2.0 (La Jolla, CA, USA). Details of the statistical methods used in the individual experiments are given in the figure legends. Statistical significance and *p*-values were calculated by a paired student's t-test, assuming normal Gaussian distribution and equal standard deviation, based on our experience in similar experiments. For *p*-values above 0.05, differences between groups were considered not significant (ns). If *p* was smaller than 0.05, differences between groups were considered significant (* $p \leq 0.05$, ** $p \leq 0.01$, **** $p \leq 0.0001$). Please note that not all formal requirements for the paired student's t-test are achieved in our setting: Gaussian distribution could not be tested due to our limited sample size. Nevertheless, it can be assumed that the t-test is quite robust (53, 54).

Results

CD80 expression by tumor cells increases antigen-specific $CD8^+$ T-cell activation

Initially, we hypothesized that CD80 expression on tumor cells as a secondary co-stimulatory signal would increase their capacity of antigen-specific activation of T-cells. Therefore, we evaluated T-cell activation in an *in vitro* co-culture experiment with CD80-transfected tumor cell lines, which presented different tumor antigens, and $CD8^+$ T cells, which expressed the matching T-cell receptor (TCR). The tumor cell lines Mel526 and A375M cells (both melanoma) and H1975 cells (non-small cell lung cancer) were electroporated with CD80-encoding mRNA, the transfection was confirmed by flow cytometry (**Fig. 1A**).

Further, the cells were loaded with tumor antigen-derived peptides. An HLA-A*02:01-restricted epitope from the melanoma antigen MelanA was used for Mel526. An HLA-A*01:01-restricted epitope from the cancer-testis antigen MAGE-A3 was used for A375M and H1975. Both melanoma lines expressed the respective antigens also endogenously. $CD8^+$ T cells from healthy donors were transfected with mRNA encoding the respective TCRs and both cell types were co-incubated overnight. T cells without a TCR were used as negative control for the cell lines that expressed the tumor antigen endogenously. The antigen-specific activation of $CD8^+$ T cells was evaluated by measuring the expression of the activation markers CD25 and CD69 by flow cytometry, and by quantifying the secretion of the cytokines IL-2, TNF, and IFNγ.

Mel526 cells which expressed CD80 induced a significantly higher proportion of $CD25^+$, $CD69^+$ and CD25/CD69 double-positive T cells compared to the non-transfected Mel526 cells (**Fig. 1B**). The endogenous expression of MelanA was enough to trigger an efficient activation of TCR-expressing T cells. Also, for A375M cells, which express the MAGE-A3 antigen, a significantly higher proportion of T cells were induced to express $CD25^+$ and $CD69^+$ when the tumor cells were expressing CD80. This was significantly measurable when the activation depended on the endogenous expression of the MAGE-A3 antigen. Tumor cells additionally loaded with the MAGE-A3 peptide further increased T-cell activation. But even here, the additional co-stimulatory effect of the CD80 expression remained, although only formally significant for the CD25/CD69 double-positive T-cell population (**Fig. 1B**). T-cell activation in the co-cultures with peptide-loaded H1975 cells was less efficient compared to the other co-cultures. Nevertheless, the expression of CD80 on H1975 cells still increased the number of $CD25^+$ and CD25/CD69 double-positive T cells significantly (**Fig. 1B**). The expression of CD80 on A375M cells that were loaded with an epitope from the melanoma antigen gp100 also increased the activation of T cells expressing the corresponding TCR (data not shown).

The secretion of IL-2, TNF, and IFNγ by the activated T cells in these co-cultures was analyzed simultaneously (**Fig. 1C**). In all tested conditions, the expression of CD80 resulted in higher concentrations of all three cytokines. This effect was significant for all cytokines in the co-cultures with MelanA peptide-loaded Mel526 cells, and for IL-2 and IFNγ in co-cultures with A375M cells, presenting both endogenous antigen and exogenous peptide (**Fig. 1C**). Despite not reaching formal significance, all other conditions displayed a similar pattern, always resulting in higher cytokine secretion when CD80 was present (**Fig. 1C**). Other cytokines, such as IL-4, IL-10, and IL-6 were also slightly increased, however with high donor variance and at much lower levels (data not shown)

These results show that different tumor cell lines indeed gain a higher capacity to activate $CD8^+$ T cells in an antigen-specific manner when co-expressing CD80. This indicates that transient transfection with CD80-encoding mRNA provides a possibility to equip tumor cells with functional co-stimulatory signaling molecules.

Tumor cells co-expressing CD80 and MelanA prime naïve $CD8^+$ T cells

Next, we examined whether CD80-transfected tumor cells gained the capability to prime and expand naïve tumor-specific $CD8^+$ T cells, which is usually an exclusive ability of professional APCs. To test this hypothesis, we performed a T-cell priming experiment. We used MelanA as a model antigen due to its high immunogenicity, its endogenous expression in Mel526 cells (see suppl. Fig. S3), and the abundance of naïve MelanA-specific T cells in most HLA-A*02:01-positive healthy donors (55). Mel526 cells were electroporated with RNA encoding CD80, and $CD8^+$ T cells were stimulated twice, each time for one week, with these Mel526 cells. Furthermore, we tested the effect of an increased antigen presentation by pulsing the Mel526 cells additionally with exogenous MelanA peptide. T cells without tumor cells served as additional control. After the 14 days of co-culture, the proportions of MelanA-specific $CD8^+$ T cells were evaluated by staining with an HLA-multimer, that consisted of the immunodominant MelanA epitope bound to HLA-A*0201. Additionally, to determine the phenotype of the MelanA-specific $CD8^+$ T cells, the surface markers CD8, CCR7, and CD45RA were evaluated by flow cytometric analysis.

The results showed that MelanA-specific $CD8^+$ T cells expanded to a percentage of 0.44% in average when stimulated with untreated Mel526 cells that endogenously express MelanA (**Fig. 2A**). The expression of CD80 significantly enhanced T-cell priming with up to 2.8 % MelanA-specific T cells in average (**Fig. 2A**). This percentage of MelanA-specific T cells is similar to that induced with MelanA-transfected professional APCs such as dendritic cells generated for application in clinical trials (NCT00074230) (56-59). Pulsing with exogenous MelanA peptide did not increase the capacity of non-transfected Mel526 cells, and the high priming capacity of the CD80-transfected cells did not further increase, indicating that the endogenous MelanA expression of Mel526 is sufficient (**Fig. 2A**). Unstimulated $CD8^+$ T cells, which had not been in contact with Mel526 cells, contained only 0.14% MelanA-specific T cells (**Fig. 2A**).

Closer examination of the MelanA-specific T cells revealed a strong shift from naïve T cells towards effector T cells for all five donors analyzed(60), as indicated by their CD45RA and CCR7 expression profile (**Fig. 2B** and **S4**). In particular, an increase in $CD45RA^-$, $CCR7^+$ T cells (indicating central memory) and a strong increase in CD45RA/CCR7 double-negative T cells (indicating effector memory) with CD80 expressing tumor cells was observed in all donors (**Fig. 2B**). For donor B and E a strong increase in $CD45RA^+$, $CCR7^-$ T cells (lytic effector) was observed, while donor A, C, and D showed only a small increase in this subtype with CD80 co-stimulation (**Fig. 2B**). The low numbers of MelanA-specific T cells stimulated with untreated Mel526 cells were mostly naïve T cells and effector memory T cells, while those left without tumor cells showed an almost completely naïve CD45RA/CCR7 double-positive phenotype (**Fig. 2B**).

Consequently, CD80 expression by tumor cells was sufficient to induce a tumor antigen-specific $CD8^+$ T-cell priming of naïve T

View Article Online
DOI: 10.1039/D5NH00667H

cells that shift towards central memory, effector memory and lytic effector T cells.

Nanoparticles encapsulating GFP-encoding mRNA transfect tumor cells

Despite the encouraging results presented above, the *in vivo* application of mRNA electroporation is challenging, if not virtually impossible. Recent advances in nanoparticle-based delivery systems, however, now provide feasible strategies for *in vivo* mRNA administration. We hypothesized that pBAE-based NPs could deliver CD80 mRNA to the tumor cells. Here we used NPs that were functionalized by adding lysine and histidine oligopeptides to the pBAE polymers to facilitate cell surface binding and endosomal escape. The resulting pBAE-based NPs were previously characterized to have a cationic surface charge of 25 to 27 mV and a hydrodynamic diameter of 140 to 160 nm, and displayed an encapsulation efficiency of 80% (61). A detailed analysis of the physiochemical features of the NPs can be found in Navalon-Lopez *et al.* and Fornaguera *et al.* (44, 61).
To visualize nanoparticle binding and distribution in tumor cells, the human cell line Mel526 was transfected with Cy5-tagged nanoparticles and analyzed over a 24-hour time course by fluorescence microscopy (**Fig. 3A**). We observed a rapid attachment of the NPs to the cell surface. Over time, the number of bright spots decreased and the signal became slightly more diffuse.
Aiming for mRNA delivery that results in functional protein expression, we investigated the ability of pBAE-based NPs, encapsulating GFP-encoding mRNA to transfect a range human tumor cell lines, including melanoma (A375M and Mel526), uveal melanoma (Mel270 and OMM2.5), non-small cell lung cancer (PC9, A549, 11-18, and H1975), Merkel cell carcinoma (MKL-1, MKL-2, and WaGa), and acute myeloid leukemia (THP-1). We compared the efficiency of mRNA electroporation with pBAE-NP transfection, the GFP expression was evaluated by flow cytometry after 24h.
The cell lines A375M, Mel526, Mel270, PC9, A549, 11-18, and H1975 were transfected with an efficiency of more than 80 % by the NPs, which was only slightly lower compared to the electroporation control (**Fig. 3B** and **3D**). In contrast, the NPs only inefficiently transfected the cell lines OMM2.5, MKL-1, MKL2, WaGa, and THP-1. Here, it has to be noted that four of these cell lines (MKL-1, MKL-2, WaGa, and THP-1) are growing in suspension, while all others are adherent cell lines. Furthermore, it was observed that the NPs showed a higher variance in their transfection ability compared to the very stable transfection rates by electroporation.
In the cell lines for which the proportions of cells transfected with NPs was similar to the electroporation control, the mean fluorescence intensity (MFI) was either similar to that of electroporated cells (Mel526 and 11-18) or appeared even higher (A375M, Mel270, PC9, A549, and H1975) (**Fig. 3C** and **3D**). The cell lines that were poorly transfected all showed low MFI when they were transfected with the NPs. Especially the Merkel cell carcinoma cell lines were transfected with lower efficiency, both by electroporation and with NPs (**Fig. 3C** and **3D**).
In general, most adherent tumor cell lines were transfected by RNA-loaded pBAE-NPs with high efficiency and expressed high levels of the mRNA-encoded GFP.

Nanoparticles as tool to deliver CD80 to tumor cells for transient expression

The promising results with GFP-encoding mRNA encouraged us to transfect a selection of the cell lines with CD80-encoding mRNA, delivered by pBAE-based NPs. We hypothesized that the duration and intensity of the CD80 expression in tumor cells might differ from that observed after electroporation (Fig. 1A), as the uptake and unpacking of the NPs clearly differs in its kinetics from the electroporation. Hence, we conducted a time course experiment with measurement at 6 h, 24 h, 48 h, and 72 h post transfection for the tumor cell lines A375M, Mel526, H1975, and WaGa and compared CD80 expression in NP-transfected cells with electroporated cells. Non-transfected and non-electroporated tumor cells served as negative control. The CD80 expression was evaluated by antibody surface staining and flow cytometry for all given time points.
In general, the transfection with NPs resulted in lower proportions of CD80-positive cells and a lower MFI compared to the CD80 mRNA-electroporated cells for all tested tumor cells lines at all time points (**Fig. 4A** and **4B**). Regarding the temporal progression, the electroporation led to a fast and even expression of CD80, with nearly 100% CD80-positive cells for all measured time points in all tumor cell lines (**Fig. 4A** left side). Here, the MFI was initially already high, peaked at 24 h and then decreased until 72h for most cell lines (**Fig. 4B** left side).
The transfection with NPs showed different temporal behavior (**Fig. 4A** right side). Initially, the percentage of CD80-positive cells was low with levels between 20% and 50% at 6 h and sharply increased reaching 40% to 80% at 24h. In Mel526 and WaGa cells, the percentage decreased again at 48 h and further at 72 h, whereas percentages in H1975 and A375M cells further increased at 48h (**Fig. 4A** right side). H1975 cells stayed at a stable proportion of 80% CD80-positive cells at 72h, while A375M cells decreased at 72h (**Fig. 4A** right side). The cellular expression levels of CD80 showed the same kinetics as the percentage of CD80-positive cells for all tumor cell lines (**Fig. 4B** right side). Of note, the suspension cell line WaGa showed in this experiment a very low proportion of CD80-positive cells and MFI also at later time points.
We concluded from this data, that the pBAE-based NPs are a feasible tool to transiently express CD80 on adherent tumor cells.

Nanoparticles induce sufficient CD80 expression in tumor cells to prime and expand T cells

Finally, we examined, whether the pBAE-NPs that contained CD80-encoding mRNA could indeed render tumor cells capable of priming and expanding naïve $CD8^+$ T cells recognizing an endogenously expressed tumor antigen. Therefore, we conducted a stimulation experiment with Mel526 cells that

View Article Online
DOI: 10.1039/D5NH00667H

endogenously express MelanA together with CD8$^+$ T cells and again made use of the fact that MelanA-specific T cells are in general naïve in healthy donors. NPs were added to the tumor cells at day 0, day 6, day 8, and day 10. At day 14, the priming and expansion of the MelanA-specific CD8$^+$ T cells was measured by HLA-multimer staining followed by flow cytometric analysis. Cultures treated with GFP mRNA-loaded NPs, tumor cells without any treatment, and T cells without tumor cells served as controls. The GFP mRNA-loaded NPs were included to distinguish any immune stimulatory effects of the NPs apart from the expression of CD80, as they are similar in chemical composition, but only encode an inert protein.

The tumor cells transfected with CD80 NPs significantly induced MelanA-specific priming of CD8$^+$ T cells with 1.4% MelanA-specific T cells in average, compared to tumor cells without treatment that induced only a very weak T-cell expansion with 0.29% MelanA-specific T cells in average (**Fig. 5A**). GFP NPs did not significantly enhance T cell priming with 0.39% MelanA-specific T cells, confirming that the priming effect is specific for CD80 and is not induced by the transfection with pBAE NPs themselves (**Fig. 5A**). In parallel to this experiment, the cytotoxicity of the CD80 NPs and GFP NPs on tumor cells was determined over a time course of 72 h. The NPs did not induce tumor cell death (**Fig. S6**).

Again, the CD45RA/CCR7 staining of the MelanA-specific T cells indicated a strong shift of naïve T cells towards effector T cells upon stimulation with CD80-transfected tumor cells for all five donors (**Fig. 5B and S6**). In all repetitions of the experiment, the strongest increase was observed for CD45RA/CCR7 double-negative T cells, indicating an effector memory phenotype. For donor A, C, D, and F, a clear increase in CD45RA$^-$, CCR7$^+$ T cells (central memory), as well as a small increase in CD45RA$^+$, CCR7$^-$ T cells (lytic effector) was observed with the CD80-transfected tumor cells (**Fig. 5B**). For Donor B, a strong increase in CD45RA$^+$, CCR7$^-$ T cells was observed with the tumor cells transfected with CD80. The GFP NPs induced in Donor B and C a small increase of effector T cells.

These results show that mRNA-based transfection of tumor cells with pBAE NPs enables them to efficiently prime naïve CD8$^+$ T cells, specific for an endogenous tumor-antigen.

CD80 expression on tumor cells during priming endows T cells with the capacity to lyse tumor cells

In a therapeutic setting, the intended function of the primed T cells would be the lysis of the tumor cells; both CD80-transfected, and CD80-negative. To determine whether priming with CD80-expressing tumor cells confers enhanced cytolytic function to T cells, we performed a chromium-based cytotoxicity assay. Therefore, Mel526 cells, either expressing CD80 or not, were labeled with chromium and co-cultured with T cells harvested on day 14 of stimulation with the tumor cells, either electroporated with CD80 RNA, or transfected with NPs containing CD80 or GFP RNA, or left untreated). The tumor cells and the T cells (effectors) were co-cultured at tumor-to-effector (T:E) ratios of 1:60, 1:20, 1:6 and 1:2. After 4h, released chromium levels in the supernatant were subsequently measured (**Fig. 6A**).

The results show that only the T cells primed with tumor cells expressing CD80, either delivered via EP or NP, were able to lyse Mel526 cells. Remarkably, these T cells demonstrated cytolytic activity against both CD80-expressing and untreated Mel526 with similar efficiency (**Fig. 6A**). No tumor cell lysis was observed at any T:E ratio when T cells had before been stimulated with untreated Mel526 or Mel526 treated with GFP-encapsulating NPs.

These results demonstrate not only that priming of T cells with CD80-expressing tumor cells provided a cytolytic capability against the exact cell type they were stimulated with but also that tumor cells without CD80 are targeted by the CD80-primed T cells, allowing also the eradication of untransfected tumor cells.

T cells primed with CD80 expressing tumor cells express less checkpoint inhibitors

Tumor cells can induce the expression of checkpoint receptors on T cells upon stimulation. To address this issue, we evaluated the expression of the checkpoint molecules PD-1 and CTLA-4 on the MelanA specific T cells. We harvested the T cells on day 14 after stimulation and performed MelanA tetramer staining along with antibody staining for PD-1 and CTLA-4 for flow cytometric analysis (**Fig. 6B**). Our results demonstrate that MelanA-specific T cells primed with CD80-expressing tumor cells exhibited significantly lower levels of PD-1 and CTLA-4 compared to those primed with untreated or GFP-transfected tumor cells (**Fig. 6B**). After priming with untreated Mel526, 30-90% of the MelanA-specific T cells expressed PD-1. Similar levels were observed when tumor cells had been treated with GFP NPs, resulting in 20-80% PD-1 expression. In contrast, electroporation with CD80 RNA reduced PD-1 expression to 2-20% by MelanA specific T cells. Similarly, CD80 nanoparticle treatment led to a reduction of PD-1 expression, with an average of approximately 20%. A similar expression pattern was observed for CTLA-4. After priming with untreated Mel526 cells or GFP-treated Mel526 cells an average of 34% or 29% of MelanA-specific T cells expressed CTLA-4, respectively. In contrast, CD80 electroporation of the tumor cells reduced CTLA-4 expression to nearly undetectable levels in all six donors. Likewise, CD80 nanoparticle treatment showed a similar effect, resulting in an average of approximately 5% CTLA-4 expression in MelanA-specific T cells. (**Fig. 6B**)

These results indicate that the functional differences observed earlier in the cytolytic activity of the CD80-primed T cells can be expanded to the expression of checkpoint molecules. Priming of T cells with CD80-expressing tumor cells induced are functionally more active T cell phenotype indicated by a low expression of inhibitory checkpoint molecules.

Transfection of Mel526 tumor spheroids *in vitro* and *in ovo*

Since we observed that tumoral CD80 expression would be beneficial, we next assessed whether the pBAE NPs also could efficiently transfect Mel526 tumor spheroids, which resemble

View Article Online
DOI: 10.1039/D5NH00667H

tumors in a 3D setting. To this end, tumor spheroids were generated and transfected with GFP mRNA pBAE nanoparticles for different time periods (24 h, 48 h, and 72 h). After transfection, spheroids were either directly analyzed by fluorescence microscopy or dissociated into single-cell suspensions for flow cytometric analysis. We observed penetration and transfection with GFP by fluorescence microscopy (**Fig. 7A**). The quantitative analysis by flow cytometry further demonstrated efficient transfection of tumor spheroids and the expression remained stable over 72 hours for GFP and CD80 (**Fig. 7B**). Interestingly, GFP and CD80 expression exhibited different kinetics. GFP expression was initially low but increased over time, whereas CD80 expression was high at early time points and decreased over time. Nevertheless, these results demonstrate that tumor spheroids can also be successfully transfected to express the surface molecule CD80.

Safety and biodistribution of pBAE NPs in general have already been demonstrated in mice previously (44). To further confirm the transfection efficacy of these pBAE NPs in human tumor cells we utilized an *in ovo* tumor model by implanting Mel526 tumor spheroids into the chorioallantoic membrane of fertilized chicken eggs. After five days of growth the spheroids were vascularized (**Fig. S8**). The tumors were treated with GFP mRNA-loaded pBAE nanoparticles for 32 hours, while control spheroids remained untreated. The tumors were then excised and directly analyzed by fluorescence microscopy. The results demonstrate that pBAE nanoparticles can transfect vascularized Mel526 tumor spheroids *in ovo* (**Fig. 7C**).

This proof-of-principle opens the avenue to bring CD80-based therapies to clinical application, where a tumor might be repetitively inoculated with the CD80-encapsulating NPs. The tumor cells induce involuntarily a robust and specific T cell activation thus turning themselves into a therapeutic anti-tumor vaccine.

Discussion

In this study, we show that equipping tumor cells with CD80 increases their ability to stimulate $CD8^+$ T cells in an antigen-specific manner. Especially the tumor cells' capacity to prime and expand naïve T cells was clearly enhanced. This demonstrates the potency of CD80 expression in tumor immunotherapy. To allow for *in vivo* transfection with CD80, we showed that pBAE-NPs containing CD80-encoding mRNA are capable of transfecting tumor cells and equip them with CD80, resulting again in an enhanced capacity to prime and expand naïve T cells, capable of lysing parental tumor cells. Moreover, T cells primed with CD80-expressing tumor cells displayed reduced levels of checkpoint inhibitors compared to those primed in absence of CD80.

Stimulation assays with TCR-transfected T cells showed that the tumor-intrinsic expression of the respective antigens was enough to observe this effect, and exogenous peptide loading only marginally increased T-cell activation. Only when the target cell lines did not express the antigen, exogenous peptide loading was required. However, the use of bulk $CD8^+$ T cells in our *in vitro* experiments may underestimate the effect of CD80, because these T cells represent a mixture of different T cell subtypes, including many which cannot respond to CD80 because they do not express CD28. In fact, expression of CD28 is restricted to naïve T cells (62, 63) and parts of the memory compartment, where its expression is gradually lost (64). Nevertheless, the expression of the pro-inflammatory cytokines IL-2, TNF, and IFNγ was highly dependent on the presence of CD80. The immunodominant HLA-A*02:01-restricted epitope from the melanoma antigen MelanA has the extraordinary feature to be recognized by a high number of naïve T cells in healthy donors (65). This allows to analyze the efficiency of APCs to prime and expand naïve T cells. In respective priming experiments, the naïve T cells that were exposed to CD80-expressing tumor cells were indeed effectively activated. These antigen-specific naïve T cells strongly proliferated to numbers which are within the same range or even higher than those observed in stimulation experiments with dendritic cells, intended for the use in tumor vaccination trials (56-59). The expanded T cells differentiated towards a memory and effector phenotype only upon receiving the CD28-activating signal. This emphasizes the potential of a CD80-based therapeutic approach to induce an efficient differentiation of the patient's reservoir of naïve T cells into tumor-specific T cells expressing a memory marker profile and capable of lysing tumor cells.

The intended application of this strategy *in vivo* depends on a successful delivery of CD80 mRNA to the tumor cells to activate anti-tumor T cells specifically. Using a biocompatible and biodegradable non-viral delivery system could be advantageous in terms of safety, if efficient. In this context, and as demonstrated previously, pBAE NPs accomplish these required attributes. Thus, a possible mode of delivery could be a transfection with pBAE NPs that contain CD80 mRNA. When comparing the transfection with GFP-RNA using these NPs or electroporation, the transfection rate was slightly lower with NPs than with electroporation and the amount of protein per cell was higher compared to electroporation for most cell types. In contrast to that, the percentage of positive cells and the intensity of expression for CD80 was considerably lower than with GFP. The NPs of CD80 and GFP were equally in quality control measurements (size and PDI), so we assume that the transfection itself works equally well for both. However, the differences of mRNA expression might be caused by the different kinetics of the transfection. The electroporation allows entry of a large amount of mRNA in a period of time in millisecond range, while the uptake of the NPs can protract over the whole incubation time (here 24h). While the GFP mRNA is a very stable protein in the cytosol, CD80 needs to be shuttled to the surface of the cell and may underlie intracellular degradation mechanisms, preventing its accumulation. In general, the NPs show a sustained transfection kinetics, as compared to electroporation and offer the advantage of a therapeutic tool that is able to exert an effect over several days after in vivo administration. Nevertheless, the question remained whether the expression levels of CD80 were enough to trigger the intended effect.

The potential of using pBAE NPs as a therapeutic strategy to deliver CD80 mRNA to tumor was demonstrated in the stimulation of T cells with NP-transfected tumor cells. The mRNA amount shuttled by the pBAE NPs as well as the transfection rate was indeed sufficient to prime naïve T cells. The transfection of the pBAE polymers itself did not alter the tumor cells in a way that they appear more immunogenic, since GFP mRNA encapsulating NPs did not enhance the priming of T cells. Accordingly, the pBAE polymers were confirmed as safe and immune-inert. Therefore, our study shows that a NP-mediated delivery of CD80 mRNA to tumor cells is a suitable therapeutic strategy to activate T cells tumor-specifically and to induce a differentiation of naïve T cells towards effector T cells and lytic T cells. Repetitive applications of the NPs may even further increase the number of tumor-specific T cells, as long as there are tumor cells left. Notably, the measured T-cell reactivity was only analyzed for the one model epitope from the antigen MelanA, which represents only a very small fraction of the whole ligandome of tumor cells. This implies that T cells could react towards multiple antigens simultaneously in patients and the co-expression of CD80 on the tumor cells could facilitate a more potent T-cell activation for all of these antigens creating a multi-faceted anti-tumor immune response. The advantage here would be that all relevant tumor-associated antigens, i.e., those efficiently presented by the tumor cells, become vaccination antigens, thus possibly inducing a broad and relevant anti-tumor reaction. Additionally, more than one of these antigens can be co-encapsulated together in a single pBAE NP formulation, making the therapeutic strategy robust, versatile and clinically feasible.

Even though we could show the benefit of CD80 expression in cell culture models, the benefit of CD80-expression in real tumors *in vivo* is a controversial topic. While a large body of research indicates a clear benefit of CD80-expression within tumors and on tumor cells, others observed that some tumors benefit from CD80 expression (reviewed by Li *et al.* (66)). As solid tumors are usually not of hematopoietic origin, one would not expect endogenous CD80 expression on the tumor cells, however infiltrating immune cells may express CD80 at high levels. This must be kept in mind, when expression levels are determined by bulk RNA sequencing. Immune histology showed CD80 expression on the tumor cells in renal cancer (67) and melanoma (68) but expression levels did not correlate with clinical outcome. In contrast, in nasopharyngeal carcinoma (69), gastric adenocarcinoma (70), and thymic epithelial tumors (71) , expression on the tumor cells was clearly correlated with a better outcome and with beneficial tumor features such as T-cell infiltration and immune activity. Work relying only on RNA sequencing data from large cohorts of patients also showed a clear association with better outcome and survival for lung adenocarcinoma (72). In breast cancer, CD80 expression on bulk RNA level was associated with immune infiltration and inflammation, but thus also correlated with immune checkpoint expression (73). In pancreatic ductal adenocarcinoma, CD80 was clearly co-expressed with immune checkpoint markers in high-risk patients (74). These conflicting results may be associated with CD80 expression levels. Low level expression seems to help tumors escape immune responses in contrast to the complete absence of expression, while high level of CD80 seem to be associated with better immune-related tumor rejection. Tirapu *et al.* showed that the expression of CD80 at low levels could act as immune escape mechanism in a murine colon cancer model (75). Marchiori *et al.* showed in contrast that knockdown of CD80 increased tumor development of colorectal cancer in mice (76). Ikeda *et al.* showed that high CD80 expression not only correlated with better survival and T-cell infiltration in thymic epithelial tumor patients, but also showed that CD80-transgenic tumor cells improved the response to immune checkpoint blockade in mice and induced formation of an effective anti-tumor T-cell response much in line with our observations (71). However, specific tumors may gain other aggressive features from CD80-mediated inflammation. For example, Kang *et al.* showed that CD80 drives migration and epithelial–mesenchymal transition, traits clearly associated with poor outcome. In summary, high CD80 expression on tumor cells usually mediates better outcome by improving T-cell infiltration and formation of anti-tumor immune responses, but low level of CD80 or special characteristics of certain tumor entities may result in worsening of the clinical outcome.

In our study, none of the CD80-transfected human tumor cell lines endogenously expressed CD80 shown by antibody staining and we confirmed that the induction of a high expression of CD80 by tumor cells enhanced anti-tumoral immune responses. In a seminal publication, Habeeth et al. showed the feasibility of *in vivo* transfection with CD80 in the murine system. They employed charge-altering releasable transporters (CART) functionalized with difluoroboron-beta-diketonate fluorophore (BDK) (77). This BDK-CART-mRNA delivery platform was utilized to deliver immunomodulatory molecules - including *CD70, OX40L, CD80, CD86, IL-12*, and *IFNγ* - in various combinations. Using a two-tumor model, they demonstrated that local administration of mRNA coding these immunomodulatory molecules can induce a systemic immune response capable of eradicating both the treated (local) tumor and untreated (distal) tumors. The observed abscopal effect is attributed to the migration of locally activated immune cells from the tumor site to the lymph nodes. Nonetheless, the study primarily focused on tumor growth monitoring. Although one T cell and one NK cell activation marker as well as cytokine concentrations within the TME were evaluated, the mechanistic basis of the observed effects remained largely unaddressed. By contrast, using a human model, we show the direct impact of CD80 expression of tumor cells on the functionality of $CD8^+$ T cells and offer a mechanistic rationale for the therapeutic efficacy observed.

Importantly, when it comes to CD80 co-stimulation a valid concern is its binding to the checkpoint molecule CTLA-4 (cytotoxic T-lymphocyte-associated Protein 4). CTLA-4 is only expressed on activated T cells and functions as inhibitory molecule to attenuate T-cell responses (78, 79). The intracellular signaling of CTLA-4 induces inhibition of TCR/CD3 (80), NF-κB and AP-1 signaling (81, 82), as well as IL-2 production (83). Furthermore, CTLA-4 has a higher affinity to CD80 than CD28. Therefore, it is assumed that CTLA-4/CD80 binding

outcompetes CD80/CD28 binding which oppresses its activating effects (84). Additionally, CTLA-4 can remove CD80 from the expressing cell by trans-endocytosis (78, 85). Tumor cells take advantage of CTLA-4 signaling to inhibit T-cell activation which paved the way for checkpoint inhibitor therapy (86). However, in our experiments, we could not observe an inhibitory effect; quite the opposite, CD80 stimulation highly induced T-cell activity while maintaining low expression of both CTLA-4 and PD-1 over a time period of 14 days. Although this was unexpected at first site, Zhao *et al.* provided compelling evidence elucidating a possible underlying mechanism using complex *in vitro* experiments (87). Specifically, the interaction of PD-L1 and CD80 in cis, that is, on the same cell, exerts distinct effects on the signaling pathways of CD80, CD28, CTLA-4, PD-L1, and PD-1. Firstly, PD-L1:CD80 interaction prevents PD-L1 from signaling via PD-1: when CD80 was co-expressed with PD-L1 on the same cell, PD-1 clustering on T cells was not observed, whereas TCR clustering remains intact. In contrast, the PD-L1:CD80 heterodimer was fully capable of activating CD28 signaling. Moreover, the authors were able to show that PD-L1:CD80 cis interaction inhibited CD80:CTLA-4 interaction. This finding is particularly notably because CTLA-4 and CD28 bind to the same conserved motif of CD80, yet CD28 binding remained unaffected. The underlaying explanation was that CD80:CTLA-4 interactions are largely driven by an avidity effect, requiring clustering of CD80 molecules to engage clustered CTLA-4 molecules. However, interaction with PD-L1 in cis was shown to prevent CD80 clustering. Overall, these findings indicate that CD80 does not solely function as activating ligand via CD28 engagement; but in addition, the PD-L1:CD80 heterodimer simultaneously neutralizes inhibitory signaling mediated by both the PD-L1:PD-1 axis and CD80:CTLA-4 axis. This mechanism is exploited through the artificial expression of CD80 in combination with the endogenous expression of PD-L1 on tumor cells (Fig. S3B). This, however, demands further investigation, especially with PD-L1-negative tumor cells. Moreover, we are aware of the fact that within the tumor microenvironment, T cells face multiple inhibitory signals and might be exhausted already. Hence, the combination of the CD80 vaccine with checkpoint inhibitors might be a feasible option for activating anti-tumoral T cells in cancer patients.

Conclusions

Although the CD80-based treatment idea has been proposed decades ago and was pursued since then (24, 25, 77), only recent developments in *in vivo* delivery systems have opened up the possibility for a safe delivery of CD80 mRNA to tumor cells. Effective mRNA delivery remains a major technical barrier, only successfully overcome by a few approaches, including lipid nanoparticles (LNPs), charge-altering releasable transporters (CARTs), and a few other systems. Additionally, it is worth remarking that although in the current article, no *in vivo* experiments could be performed, our previous studies validated the transference of pBAE NPs results from *in vitro* to *in vivo*. These NPs could even be administered intra-tumorally and induce effective anti-tumor immune responses right at the location of action. This proof-of-concept study shows that the exploration of the combination of relatively old ideas with new technologies enables new therapeutic strategies to find new off-the-shelf treatment options that are effective, affordable, and safe.

Author contributions

AKB,FB and NF performed the experiments, AT-C, CF, and SB invented and generated the pBAE NPs, AKB, FB and SK analyzed the data and designed the figures. JD, CF, and NS conceptualized the study. JD, SB, and CF acquired funding. AKB, FB, and JD wrote the draft of the manuscript. All authors were involved writing the final manuscript. All authors have read and approved the final manuscript.

Conflicts of interest

All authors declare that the research was conducted in the absence of any commercial or financial relationships that could be construed as a potential conflict of interest.

Data availability

The data supporting this article have been included as part of the Supplementary Information.

Funding

This work was supported by the transnational joint research program ERA-NET TRANSCAN, Project TumorOUT (BMBF funding number 01KT2305A) to JD and from MICIN/AEI (MCIN/AEI/10.13039/501100011033/FEDER, UE and FCAECC (TRNSC213882FORN) to CF). This work was also supported by the Deutsche Forschungsgemeinschaft (DFG, German Research Foundation) by the Research Training Group GRK2504/1 (project number 401821119), research project B4 to JD.

Acknowledgements

Cristina Fornaguera acknowledge the ICREA Academia 2024 recognition, from AGAUR-Generalitat de Catalunya, for their financial support of her research. We thank Nadine Hellmuth and Annett Hamann for their helpful technical assistance, and Ignasi Espinós i Longa for his help in establishing the NP production in Erlangen. We thank the medical staff from the department of Dermatology of the Uniklinikum Erlangen, especially Dr. Elias Koch for their support with all blood donations. Furthermore, we would like to thank all voluntary blood donors. We also want to express our gratitude towards Jürgen Becker, Hinrich Abken, Corlien Aarnoudse, Martine Jager, Markus Biburger, and Rafael Rosell for providing us all the different cell lines.

References

1. Bottcher JP, Reis e Sousa C. The Role of Type 1 Conventional Dendritic Cells in Cancer Immunity. Trends Cancer. 2018;4(11):784-92.

2. Dominiak A, Chelstowska B, Olejarz W, Nowicka G. Communication in the Cancer Microenvironment as a Target for Therapeutic Interventions. Cancers (Basel). 2020;12(5).

3. Landskron G, De la Fuente M, Thuwajit P, Thuwajit C, Hermoso MA. Chronic inflammation and cytokines in the tumor microenvironment. J Immunol Res. 2014;2014:149185.

4. Schreiber RD, Old LJ, Smyth MJ. Cancer immunoediting: integrating immunity's roles in cancer suppression and promotion. Science. 2011;331(6024):1565-70.

5. Thommen DS, Schumacher TN. T Cell Dysfunction in Cancer. Cancer Cell. 2018;33(4):547-62.

6. Tucci M, Passarelli A, Mannavola F, Felici C, Stucci LS, Cives M, et al. Immune System Evasion as Hallmark of Melanoma Progression: The Role of Dendritic Cells. Front Oncol. 2019;9:1148.

7. Whiteside TL. Immune suppression in cancer: effects on immune cells, mechanisms and future therapeutic intervention. Semin Cancer Biol. 2006;16(1):3-15.

8. Thommen DS, Schreiner J, Muller P, Herzig P, Roller A, Belousov A, et al. Progression of Lung Cancer Is Associated with Increased Dysfunction of T Cells Defined by Coexpression of Multiple Inhibitory Receptors. Cancer Immunol Res. 2015;3(12):1344-55.

9. Yu X, Harden K, Gonzalez LC, Francesco M, Chiang E, Irving B, et al. The surface protein TIGIT suppresses T cell activation by promoting the generation of mature immunoregulatory dendritic cells. Nat Immunol. 2009;10(1):48-57.

10. Freeman GJ, Freedman AS, Segil JM, Lee G, Whitman JF, Nadler LM. B7, a new member of the Ig superfamily with unique expression on activated and neoplastic B cells. J Immunol. 1989;143(8):2714-22.

11. Geppert TD, Davis LS, Gur H, Wacholtz MC, Lipsky PE. Accessory cell signals involved in T-cell activation. Immunol Rev. 1990;117:5-66.

12. Chen L, Flies DB. Molecular mechanisms of T cell co-stimulation and co-inhibition. Nat Rev Immunol. 2013;13(4):227-42.

13. Boesteanu AC, Katsikis PD. Memory T cells need CD28 costimulation to remember. Semin Immunol. 2009;21(2):69-77.

14. Bromley SK, Iaboni A, Davis SJ, Whitty A, Green JM, Shaw AS, et al. The immunological synapse and CD28-CD80 interactions. Nat Immunol. 2001;2(12):1159-66.

15. van der Merwe PA, Bodian DL, Daenke S, Linsley P, Davis SJ. CD80 (B7-1) binds both CD28 and CTLA-4 with a low affinity and very fast kinetics. J Exp Med. 1997;185(3):393-403.

16. Kane LP, Lin J, Weiss A. It's all Rel-ative: NF-kappaB and CD28 costimulation of T-cell activation. Trends Immunol. 2002;23(8):413-20.

17. Michel F, Mangino G, Attal-Bonnefoy G, Tuosto L, Alcover A, Roumier A, et al. CD28 utilizes Vav-1 to enhance TCR-proximal signaling and NF-AT activation. J Immunol. 2000;165(7):3820-9.

18. Rincon M, Flavell RA. AP-1 transcriptional activity requires both T-cell receptor-mediated and co-stimulatory signals in primary T lymphocytes. EMBO J. 1994;13(18):4370-81.

19. Boise LH, Minn AJ, Noel PJ, June CH, Accavitti MA, Lindsten T, et al. CD28 costimulation can promote T cell survival by enhancing the expression of Bcl-XL. Immunity. 1995;3(1):87-98.

20. Jenkins MK, Taylor PS, Norton SD, Urdahl KB. CD28 delivers a costimulatory signal involved in antigen-specific IL-2 production by human T cells. J Immunol. 1991;147(8):2461-6.

21. Thompson CB, Lindsten T, Ledbetter JA, Kunkel SL, Young HA, Emerson SG, et al. CD28 activation pathway regulates the production of multiple T-cell-derived lymphokines/cytokines. Proc Natl Acad Sci U S A. 1989;86(4):1333-7.

22. Frauwirth KA, Alegre ML, Thompson CB. Induction of T cell anergy in the absence of CTLA-4/B7 interaction. J Immunol. 2000;164(6):2987-93.

23. Wells AD, Walsh MC, Bluestone JA, Turka LA. Signaling through CD28 and CTLA-4 controls two distinct forms of T cell anergy. J Clin Invest. 2001;108(6):895-903.

24. Kaufmann AM, Gissmann L, Street D, Schreckenberger C, Hunter M, Qiao L. Expression of CD80 enhances immunogenicity of cervical carcinoma cells in vitro. Cell Immunol. 1996;169(2):246-51.

25. Dunussi-Joannopoulos K, Weinstein HJ, Nickerson PW, Strom TB, Burakoff SJ, Croop JM, et al. Irradiated B7-1 transduced primary acute myelogenous leukemia (AML) cells can be used as therapeutic vaccines in murine AML. Blood. 1996;87(7):2938-46.

26. Guckel B, Stumm S, Rentzsch C, Marme A, Mannhardt G, Wallwiener D. A CD80-transfected human breast cancer cell variant induces HER-2/neu-specific T cells in HLA-A*02-matched situations in vitro as well as in vivo. Cancer Immunol Immunother. 2005;54(2):129-40.

27. Dols A, Smith JW, 2nd, Meijer SL, Fox BA, Hu HM, Walker E, et al. Vaccination of women with metastatic breast cancer, using a costimulatory gene (CD80)-modified, HLA-A2-matched, allogeneic, breast cancer cell line: clinical and immunological results. Hum Gene Ther. 2003;14(11):1117-23.

28. Schmidt-Wolf IG, Hauser S, Weikert S, Grünwald V, Schroff M, Schmidt M, et al. The Novel Cancer Vaccine, Consisting of Genetically Modified Allogeneic Tumor Cells and Immunomodulator Mgn1601: Updated Results of a Phase 1-2 Study in Patients with Advanced Renal Cell Carcinoma. Annals of Oncology. 2012;23:268-.

29. Volz B, Schmidt M, Heinrich K, Kapp K, Schroff M, Wittig B. Design and characterization of the tumor vaccine MGN1601, allogeneic fourfold gene-modified vaccine cells combined with a TLR-9 agonist. Mol Ther Oncolytics. 2016;3:15023.

30. Lorentzen C, Haanen J, Met Ö, Svane I. Correction to Lancet Oncol 2022; 23: e450-58. Lancet Oncol. 2022;23(11):e492.

31. Liu C, Shi Q, Huang X, Koo S, Kong N, Tao W. mRNA-based cancer therapeutics. Nat Rev Cancer. 2023;23(8):526-43.

32. Morse DE, Yanofsky C. Polarity and the degradation of mRNA. Nature. 1969;224(5217):329-31.

33. Wang C, Liu H. Factors influencing degradation kinetics of mRNAs and half-lives of microRNAs, circRNAs, lncRNAs in blood in vitro using quantitative PCR. Sci Rep. 2022;12(1):7259.

34. Guan S, Rosenecker J. Nanotechnologies in delivery of mRNA therapeutics using nonviral vector-based delivery systems. Gene Ther. 2017;24(3):133-43.

35. Kranz LM, Diken M, Haas H, Kreiter S, Loquai C, Reuter KC, et al. Systemic RNA delivery to dendritic cells exploits antiviral defence for cancer immunotherapy. Nature. 2016;534(7607):396-401.

36. Alameh MG, Tombacz I, Bettini E, Lederer K, Sittplangkoon C, Wilmore JR, et al. Lipid nanoparticles enhance the efficacy of mRNA and protein subunit vaccines by inducing robust T follicular helper cell and humoral responses. Immunity. 2021;54(12):2877-92 e7.

37. Zhong S, Breton B, Zheng W, McFadyen I, Hopson K, Frederick J, et al. Abstract 6539: Bioinformatics algorithm of mRNA-4157 identifies neoantigens with pre-existing TIL reactivities in colorectal tumors. Cancer Research. 2020;80(16_Supplement):6539-.

38. Sayour EJ, Grippin A, De Leon G, Stover B, Rahman M, Karachi A, et al. Personalized Tumor RNA Loaded Lipid-Nanoparticles Prime the Systemic and Intratumoral Milieu for Response to Cancer Immunotherapy. Nano Lett. 2018;18(10):6195-206.

39. Yaremenko AV, Khan MM, Zhen X, Tang Y, Tao W. Clinical advances of mRNA vaccines for cancer immunotherapy. Med. 2025;6(1):100562.

40. Pan S, Fan R, Han B, Tong A, Guo G. The potential of mRNA vaccines in cancer nanomedicine and immunotherapy. Trends Immunol. 2024;45(1):20-31.

41. Shi D, Beasock D, Fessler A, Szebeni J, Ljubimova JY, Afonin KA, et al. To PEGylate or not to PEGylate: Immunological properties of nanomedicine's most popular component, polyethylene glycol and its alternatives. Adv Drug Deliv Rev. 2022;180:114079.

42. Riera R, Tauler J, Feiner-Gracia N, Borros S, Fornaguera C, Albertazzi L. Complex pBAE Nanoparticle Cell Trafficking: Tracking Both Position and Composition Using Super Resolution Microscopy. ChemMedChem. 2022;17(13):e202100633.

43. Fornaguera C, Diaz-Caballero M, Garcia-Fernandez C, Olmo L, Stampa-Lopez Pinto M, Navalon-Lopez M, et al. Synthesis and Characterization of mRNA-Loaded Poly(Beta Aminoesters) Nanoparticles for Vaccination Purposes. J Vis Exp. 2021(174).

44. Fornaguera C, Guerra-Rebollo M, Angel Lazaro M, Castells-Sala C, Meca-Cortes O, Ramos-Perez V, et al. mRNA Delivery System for Targeting Antigen-Presenting Cells In Vivo. Adv Healthc Mater. 2018;7(17):e1800335.

45. Fornaguera C, Torres-Coll A, Olmo L, Garcia-Fernandez C, Guerra-Rebollo M, Borros S. Engineering oncogene-targeted anisamide-functionalized pBAE nanoparticles as efficient lung cancer antisense therapies. RSC Adv. 2023;13(43):29986-30001.

46. Garcia-Fernandez C, Virgilio T, Latino I, Guerra-Rebollo M, S FG, Borros S, et al. Stealth mRNA nanovaccines to control lymph node trafficking. J Control Release. 2024;374:325-36.

47. Kozlowski JM, Hart IR, Fidler IJ, Hanna N. A human melanoma line heterogeneous with respect to metastatic capacity in athymic nude mice. J Natl Cancer Inst. 1984;72(4):913-7.

48. Birkholz K, Hofmann C, Hoyer S, Schulz B, Harrer T, Kampgen E, et al. A fast and robust method to clone and functionally validate T-cell receptors. J Immunol Methods. 2009;346(1-2):45-54.

49. Sauerer T, Albrecht L, Sievers NM, Gerer KF, Hoyer S, Dörrie J, et al. Electroporation of mRNA as a Universal Technology Platform to Transfect a Variety of Primary Cells with Antigens and Functional Proteins. Methods Mol Biol. 2024;2786:219-35.

50. Schaft N, Dorrie J, Muller I, Beck V, Baumann S, Schunder T, et al. A new way to generate cytolytic tumor-specific T cells: electroporation of RNA coding for a T cell receptor into T lymphocytes. Cancer Immunol Immunother. 2006;55(9):1132-41.

51. Dosta P, Segovia N, Cascante A, Ramos V, Borros S. Surface charge tunability as a powerful strategy to control electrostatic interaction for high efficiency silencing, using tailored oligopeptide-modified poly(beta-amino ester)s (PBAEs). Acta Biomater. 2015;20:82-93.

52. Mapanao AK, Che PP, Sarogni P, Sminia P, Giovannetti E, Voliani V. Tumor grafted - chick chorioallantoic membrane as an alternative model for biological cancer research and conventional/nanomaterial-based theranostics evaluation. Expert Opin Drug Metab Toxicol. 2021;17(8):947-68.

53. Pagano RR. Understanding Statistics in the Behavioral Sciences. 9th ed. Belmont, CA: Wadsworth Publishing Co Inc; 2009.

54. Salkind N. Encyclopedia of Research Design. Los Angeles: Sage; 2010 12/16/2010.

55. Pittet MJ, Zippelius A, Valmori D, Speiser DE, Cerottini JC, Romero P. Melan-A/MART-1-specific CD8 T cells: from thymus to tumor. Trends Immunol. 2002;23(7):325-8.

56. Dorrie J, Schaft N, Muller I, Wellner V, Schunder T, Hanig J, et al. Introduction of functional chimeric E/L-selectin by RNA electroporation to target dendritic cells from blood to lymph nodes. Cancer Immunol Immunother. 2008;57(4):467-77.

57. Erdmann M, Dorrie J, Schaft N, Strasser E, Hendelmeier M, Kampgen E, et al. Effective clinical-scale production of dendritic cell vaccines by monocyte elutriation directly in medium, subsequent culture in bags and final antigen loading using peptides or RNA transfection. J Immunother. 2007;30(6):663-74.

58. Schaft N, Dorrie J, Thumann P, Beck VE, Muller I, Schultz ES, et al. Generation of an optimized polyvalent monocyte-derived dendritic cell vaccine by transfecting defined RNAs after rather than before maturation. J Immunol. 2005;174(5):3087-97.

59. Chondronasiou D, Eisden T, Stam AGM, Matthews QL, Icyuz M, Hooijberg E, et al. Improved Induction of Anti-Melanoma T Cells by Adenovirus-5/3 Fiber Modification to Target Human DCs. Vaccines (Basel). 2018;6(3).

60. Sallusto F, Lenig D, Forster R, Lipp M, Lanzavecchia A. Two subsets of memory T lymphocytes with distinct homing potentials and effector functions. Nature. 1999;401(6754):708-12.

61. Navalon-Lopez M, Dols-Perez A, Grijalvo S, Fornaguera C, Borros S. Unravelling the role of individual components in pBAE/polynucleotide polyplexes in the synthesis of tailored carriers for specific applications: on the road to rational formulations. Nanoscale Adv. 2023;5(6):1611-23.

62. Speiser DE, Valmori D, Rimoldi D, Pittet MJ, Liénard D, Cerundolo V, et al. CD28-negative cytolytic effector T cells frequently express NK receptors and are present at variable proportions in circulating lymphocytes from healthy donors and

melanoma patients. European Journal of Immunology. 1999;29(6):1990-9.

63. Mou D, Espinosa J, Lo DJ, Kirk AD. CD28 negative T cells: is their loss our gain? Am J Transplant. 2014;14(11):2460-6.

64. Tomiyama H, Matsuda T, Takiguchi M. Differentiation of human CD8(+) T cells from a memory to memory/effector phenotype. J Immunol. 2002;168(11):5538-50.

65. Pittet MJ, Zippelius A, Valmori D, Speiser DE, Cerottini JC, Romero P. Melan-A/MART-1-specific CD8 T cells: from thymus to tumor. Trends Immunol. 2002;23(7):325-8.

66. Li L, Yang L, Jiang D. Research progress of CD80 in the development of immunotherapy drugs. Front Immunol. 2024;15:1496992.

67. Floercken. Immunomodulatory molecules in renal cell cancer: CD80 and CD86 are expressed on tumor cells. 2017.

68. Bernsen MR, Hakansson L, Gustafsson B, Krysander L, Rettrup B, Ruiter D, et al. On the biological relevance of MHC class II and B7 expression by tumour cells in melanoma metastases. Br J Cancer. 2003;88(3):424-31.

69. Chang CS, Chang JH, Hsu NC, Lin HY, Chung CY. Expression of CD80 and CD86 costimulatory molecules are potential markers for better survival in nasopharyngeal carcinoma. BMC Cancer. 2007;7:88.

70. Feng XY, Lu L, Wang KF, Zhu BY, Wen XZ, Peng RQ, et al. Low expression of CD80 predicts for poor prognosis in patients with gastric adenocarcinoma. Future Oncol. 2019;15(5):473-83.

71. Ikeda H, Nagasaki J, Shimizu D, Katsuya Y, Horinouchi H, Hosomi Y, et al. Immunologic Significance of CD80/CD86 or Major Histocompatibility Complex-II Expression in Thymic Epithelial Tumors. JTO Clin Res Rep. 2023;4(10):100573.

72. Feng W, He Z, Shi L, Zhu Z, Ma H. Significance of CD80 as a Prognostic and Immunotherapeutic Biomarker in Lung Adenocarcinoma. Biochem Genet. 2023;61(5):1937-66.

73. Zhang Q, Gao C, Shao J, Zhang S, Wang P, Wang Z. Molecular and Clinical Characterization of CD80 Expression via Large-Scale Analysis in Breast Cancer. Front Pharmacol. 2022;13:869877.

74. Wang W, Yan L, Guan X, Dong B, Zhao M, Wu J, et al. Identification of an Immune-Related Signature for Predicting Prognosis in Patients With Pancreatic Ductal Adenocarcinoma. Front Oncol. 2020;10:618215.

75. Tirapu I, Huarte E, Guiducci C, Arina A, Zaratiegui M, Murillo O, et al. Low surface expression of B7-1 (CD80) is an immunoescape mechanism of colon carcinoma. Cancer Res. 2006;66(4):2442-50.

76. Marchiori C, Scarpa M, Kotsafti A, Morgan S, Fassan M, Guzzardo V, et al. Epithelial CD80 promotes immune surveillance of colonic preneoplastic lesions and its expression is increased by oxidative stress through STAT3 in colon cancer cells. J Exp Clin Cancer Res. 2019;38(1):190.

77. Haabeth OAW, Blake TR, McKinlay CJ, Tveita AA, Sallets A, Waymouth RM, et al. Local Delivery of Ox40l, Cd80, and Cd86 mRNA Kindles Global Anticancer Immunity. Cancer Res. 2019;79(7):1624-34.

78. Robinson MA, Kennedy A, Orozco CT, Chen HC, Waters E, Giovacchini D, et al. Rigid, bivalent CTA-4 binding to CD80 is required to disrupt the cis CD80/PD-L1 interaction. Cell Rep. 2024;43(9):114768.

79. Walunas TL, Lenschow DJ, Bakker CY, Linsley PS, Freeman GJ, Green JM, et al. CTLA-4 can function as a negative regulator of T cell activation. Immunity. 1994;1(5):405-13.

80. Hossen MM, Ma Y, Yin Z, Xia Y, Du J, Huang JY, et al. Current understanding of CTLA-4: from mechanism to autoimmune diseases. Front Immunol. 2023;14:1198365.

81. Harlin H, Hwang KW, Palucki DA, Kim O, Thompson CB, Boothby M, et al. CTLA-4 engagement regulates NF-kappaB activation in vivo. Eur J Immunol. 2002;32(8):2095-104.

82. Olsson C, Riesbeck K, Dohlsten M, Michaelsson E. CTLA-4 ligation suppresses CD28-induced NF-kappaB and AP-1 activity in mouse T cell blasts. J Biol Chem. 1999;274(20):14400-5.

83. Krummel MF, Allison JP. CTLA-4 engagement inhibits IL-2 accumulation and cell cycle progression upon activation of resting T cells. J Exp Med. 1996;183(6):2533-40.

84. Oosterwegel MA, Greenwald RJ, Mandelbrot DA, Lorsbach RB, Sharpe AH. CTLA-4 and T cell activation. Curr Opin Immunol. 1999;11(3):294-300.

85. Qureshi OS, Zheng Y, Nakamura K, Attridge K, Manzotti C, Schmidt EM, et al. Trans-endocytosis of CD80 and CD86: a molecular basis for the cell-extrinsic function of CTLA-4. Science. 2011;332(6029):600-3.

86. Shiravand Y, Khodadadi F, Kashani SMA, Hosseini-Fard SR, Hosseini S, Sadeghirad H, et al. Immune Checkpoint Inhibitors in Cancer Therapy. Curr Oncol. 2022;29(5):3044-60.

87. Zhao Y, Lee CK, Lin CH, Gassen RB, Xu X, Huang Z, et al. PD-L1:CD80 Cis-Heterodimer Triggers the Co-stimulatory Receptor CD28 While Repressing the Inhibitory PD-1 and CTLA-4 Pathways. Immunity. 2019;51(6):1059-73 e9.

Figure Legends

Figure 1: CD80-expressing tumor cells activate CD8⁺ T cells. Tumor cells (Mel526, A375M, and H1975) were electroporated with CD80 mRNA and co-cultured with CD8⁺ T cells that express the T-cell receptor for MelanA or MAGE-A3 at a ratio of 1:1. Peptide-loaded tumor cells were used to increase the endogenous expression of the tumor antigens. (**A**) The CD80 expression on the tumor cell surface was evaluated after 24h via flow cytometry. Here, histograms of one representative experiment is shown. (**B**) T-cell activation in the co-culture was measured by the number of CD3+ cells that express the surface markers CD25 and CD69 through flow cytometry. The bar graphs depict mean values of 5 different donors for Mel526 (MelanA), 4 donors for A375M (MAGE-A3), and 3 donors for H1975 (MAGE-A3) ±SD. Statistical analysis was performed with a paired t-test, *:p<0.05. (C) The supernatants of the co-cultures were analyzed for the secreted cytokines. Mean values ±SD of the concentrations of IL-2, TNF, and IFNγ after co-culture with Mel526 (5 donors), A375M (4 donors), and H1975 (3 donors) are depicted. Statistical analysis was performed with a paired t-test, *:p<0.05.

Figure 2: Priming assay with electroporated tumor cells. Per condition, 10^6 CD8+ T cells of HLA-A*02:01 donors were co-cultured with 10^5 Mel526 cells either untreated or loaded with MelanA peptide (+/- peptide) and either not electroporated or electroporated with CD80 mRNA (+/- CD80). T cells without tumor cells served as control. At day 7, the T cells were re-stimulated with Mel526 +/- peptide and +/- CD80 as in the initial setup. At day 14 of co-incubation, the cells were harvested and a MelanA MHC-dextramer staining combined with an antibody staining for CD8, CCR7, and CD45RA was conducted. (**A**) Depicted is the percentage of MelanA-specific T cells in the different Mel526 conditions described above for 5 donors. Statistical analysis was performed with a paired t-test, *:p<0.05. Analyzed conditions were not significantly different if not stated differently. (**B**) Depicted are the subpopulations of MelanA-specific T cells in relation to the actual percentage of MelanA-specific T cells for each donor separately. T-cell subtypes are divided into naïve T cells (CD45RA / CCR7 double-positive), central memory T cells (CD45RA⁻, CCR7⁺), effector memory T cells (CD45RA/CCR7 double-negative), and lytic effector T cells (CD45⁺, CCR7⁻).

Figure 3: Nanoparticles transfect cell lines of different tumor entities with high efficiency. For the Cy5-labeled nanoparticle (Cy5 NP) transfection assay, Mel526 cells were seeded prior to transfection. Cy5 NPs were then added and imaging was initiated immediately. (A) Representative images from a selected region of interest are shown for the Cy5 fluorescence channel (top), brightfield channel (middle), and the corresponding overlays (bottom) at the indicated time points (0 h, 2 h, 4 h, and 24 h). The tumor cell lines A375M, Mel526, Mel270, OMM2.5, PC9, A549, 11-18, H1975, MKL-1, MKL-2, WaGa, and THP1 were transfected with RNA coding for GFP either by electroporation (EP) or by nanoparticles (NP). The (**B**) proportion of GFP-positive cells and the (**C**) mean fluorescence intensity (MFI) was determined by flow cytometry 24 h after transfection. The mean ±SD of 3 independent experiments is depicted. (**D**) Histograms of GFP expression after transfection with NP and electroporation of the cell lines listed above for one representative experiment. Unstained controls are depicted by the black line and colorless filling.

Figure 4: CD80 expression in different tumor cell lines over 72 hours. CD80 mRNA was delivered via electroporation or nanoparticles (NP) transfection to the tumor cell lines A375M (purple), H1975 (green), Mel526 (blue), and WaGa (red). (**A**) Depicted is the percentage of CD80 positive (CD80+) tumor cells of the referring cell line after 6 h, 24 h, 48 h, and 72 h as mean ±SD conducted in 3 independent experiments. (**B**) shows the delta mean fluorescence intensity (ΔMFI) of CD80 positive (CD80⁺) single cells for the experiment (A).

Figure 5: Priming assay with nanoparticle treated tumor cells. Per condition, 10^6 CD8⁺ T cells of HLA-A*02:01 donors were co-cultured with 10^5 Mel526 cells either untreated (-), treated with CD80 RNA-encapsulating nanoparticles (NP CD80) or GFP mRNA-encapsulating nanoparticles (NP GFP). NPs were added at day 0, day 6, day 8, and day 10 to the co-culture. T cells without tumor cells served as control. At day 14 of the co-incubation, the cells were harvested and a MelanA MHC-tetramer staining, as well as an antibody staining for CD8, CCR7, and CD45RA was conducted. (**A**) Depicted is the percentage of MelanA-specific T cells in the different Mel526 conditions described above for 5 donors. Statistical analysis was performed with a paired t-test, **=p<0.01, ns=not significant. (**B**) Depicted are the subpopulations of MelanA-specific T cells in relation to the actual percentage of MelanA-specific T cells for each donor separately. T-cell subtypes are divided into naïve T cells (CD45RA/CCR7 double-positive), central memory T cells (CD45RA⁻, CCR7⁺), effector memory T cells (CD45RA/CCR7 double-negative) and lytic effector T cells (CD45⁺, CCR7⁻).

Figure 6: Cytotoxic potential and checkpoint expression of primed T cells. Per condition, 10^6 CD8⁺ T cells of HLA-A*02:01 donors were co-cultured with 10^5 Mel526 cells either untreated (Mel526 only), electroporated with CD80 RNA (EP CD80), treated with CD80 RNA-encapsulating nanoparticles (CD80 NP) or GFP mRNA-encapsulating nanoparticles (GFP NP). NPs were added at day 0, day 6, day 8, and day 10 to the co-culture. T cells without tumor cells served as control. At day 14 of the co-incubation, the cells were harvested and analyzed for their cytotoxic potential and expression of immune checkpoints. (**A**) In a chromium-based cytotoxicity release assay, the primed T cells (Mel526 only, EP CD80, GFP NP, CD80 NP) as effector cells were incubated with Cr51-labelled Mel526 that were either untreated or electroporated with CD80 RNA at decreasing tumor-to-effector cell ratio of 1:60, 1:20, 1:6 and 1:2. After 4h, the released Cr51 in the supernatant indicated the lysis of the tumor cells. Here, the relative lysis in % is depicted for three individual experiments. (**B**) The primed T cells were also stained with a MelanA MHC-tetramer staining and antibodies for PD-1 and CTLA-4 to determine the immune checkpoint expression on the antigen-specific T cells. The number of MelanA+ T cells expressing PD-1 or CTLA-4 are displayed for six individual donors. Statistical analysis was performed with a paired t-test, **=p<0.01, *=p<0.05, ns=not significant.

Figure 7. Transfection of Mel526 tumor spheroids *in vitro* and *in ovo*. (A) Mel526 tumor spheroids were transfected with GFP nanoparticles (NPs). Images were acquired 24 h post-transfection and non-transfected spheroids served as negative control. (B) Time course of transfection efficiency in Mel526 tumor spheroids treated with GFP mRNA pBAE NPs or CD80 mRNA pBAE NPs for 24, 48, and 72 h. Following treatment with mRNA NPs for the indicated time points, single-cell suspensions were generated by dissociated the spheroids using PBS-EDTA. Cells were subsequently analyzed for CD80 and GFP expression by flow cytometry. Spheroids incubated for similar time periods without NPs served as controls. The experiment was performed three independent times with 2–3 technical replicates each. Statistical analysis was performed with an unpaired t-test, ****=p<0.0001. (C) Mel526 tumor spheroids transplanted onto the CAM and transfected with GFP NPs *in ovo*. Spheroids were grafted onto the chorioallantoic membrane and allowed to grow for 5 days before nanoparticle treatment; control tumors remained untreated.

View Article Online
DOI: 10.1039/D5NH00667H

After 32 h, tumors were excised and imaged immediately by fluorescence microscopy. Top left: untreated tumor spheroid (brightfield). Top right: untreated tumor spheroid (GFP channel). Bottom left: GFP mRNA NP-treated tumor spheroid (brightfield). Bottom right: GFP mRNA NP-treated tumor spheroid (GFP channel).

View Article Online
DOI: 10.1039/D5NH00667H

Figure 1

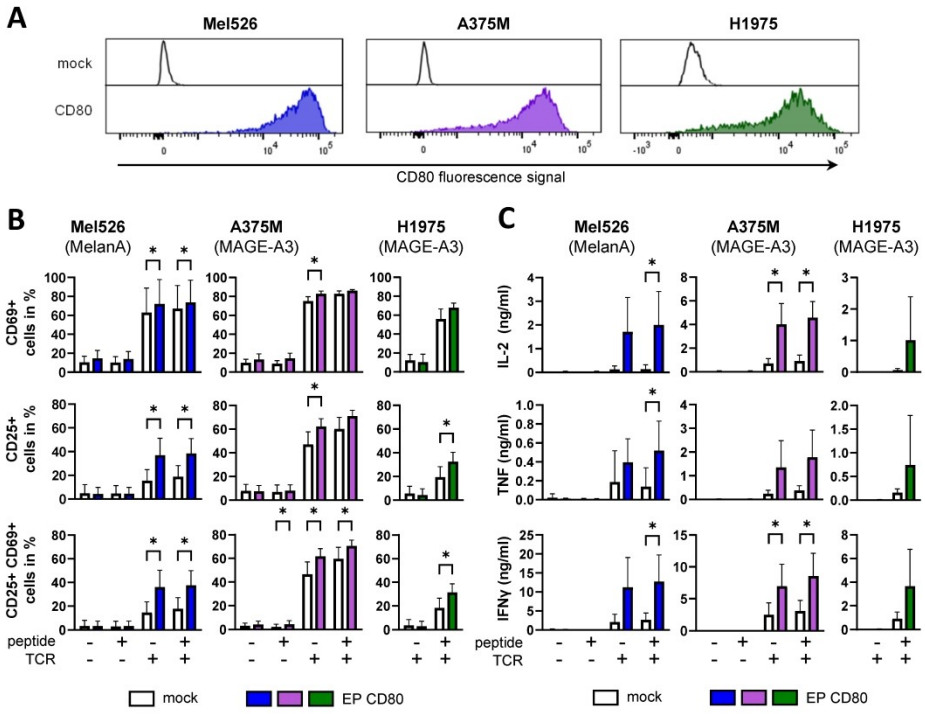

Figure 1: CD80-expressing tumor cells activate CD8+ T cells. Tumor cells (Mel526, A375M, and H1975) were electroporated with CD80 mRNA and co-cultured with CD8+ T cells that express the T-cell receptor for MelanA or MAGE-A3 at a ratio of 1:1. Peptide-loaded tumor cells were used to increase the endogenous expression of the tumor antigens. (A) The CD80 expression on the tumor cell surface was evaluated after 24h via flow cytometry. Here, histograms of one representative experiment is shown. (B) T-cell activation in the co-culture was measured by the number of CD3+ cells that express the surface markers CD25 and CD69 through flow cytometry. The bar graphs depict mean values of 5 different donors for Mel526 (MelanA), 4 donors for A375M (MAGE-A3), and 3 donors for H1975 (MAGE-A3) ±SD. Statistical analysis was performed with a paired t-test, *:$p<0.05$. (C) The supernatants of the co-cultures were analyzed for the secreted cytokines. Mean values ±SD of the concentrations of IL-2, TNF, and IFNγ after co-culture with Mel526 (5 donors), A375M (4 donors), and H1975 (3 donors) are depicted. Statistical analysis was performed with a paired t-test, *:$p<0.05$.

486x413mm (236 x 236 DPI)

View Article Online
DOI: 10.1039/D5NH00667H

Figure 2

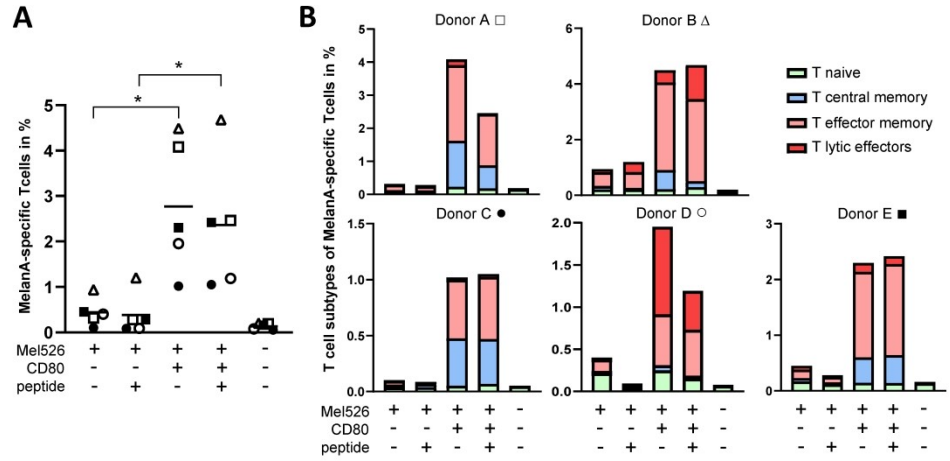

Figure 2: Priming assay with electroporated tumor cells. Per condition, 106 CD8+ T cells of HLA-A*02:01 donors were co-cultured with 105 Mel526 cells either untreated or loaded with MelanA peptide (+/- peptide) and either not electroporated or electroporated with CD80 mRNA (+/- CD80). T cells without tumor cells served as control. At day 7, the T cells were re-stimulated with Mel526 +/- peptide and +/- CD80 as in the initial setup. At day 14 of co-incubation, the cells were harvested and a MelanA MHC-dextramer staining combined with an antibody staining for CD8, CCR7, and CD45RA was conducted. (A) Depicted is the percentage of MelanA-specific T cells in the different Mel526 conditions described above for 5 donors. Statistical analysis was performed with a paired t-test, *:p<0.05. Analyzed conditions were not significantly different if not stated differently. (B) Depicted are the subpopulations of MelanA-specific T cells in relation to the actual percentage of MelanA-specific T cells for each donor separately. T-cell subtypes are divided into naïve T cells (CD45RA / CCR7 double-positive), central memory T cells (CD45RA-, CCR7+), effector memory T cells (CD45RA/CCR7 double-negative), and lytic effector T cells (CD45+, CCR7-).

481x290mm (236 x 236 DPI)

View Article Online
DOI: 10.1039/D5NH00667H

Figure 3

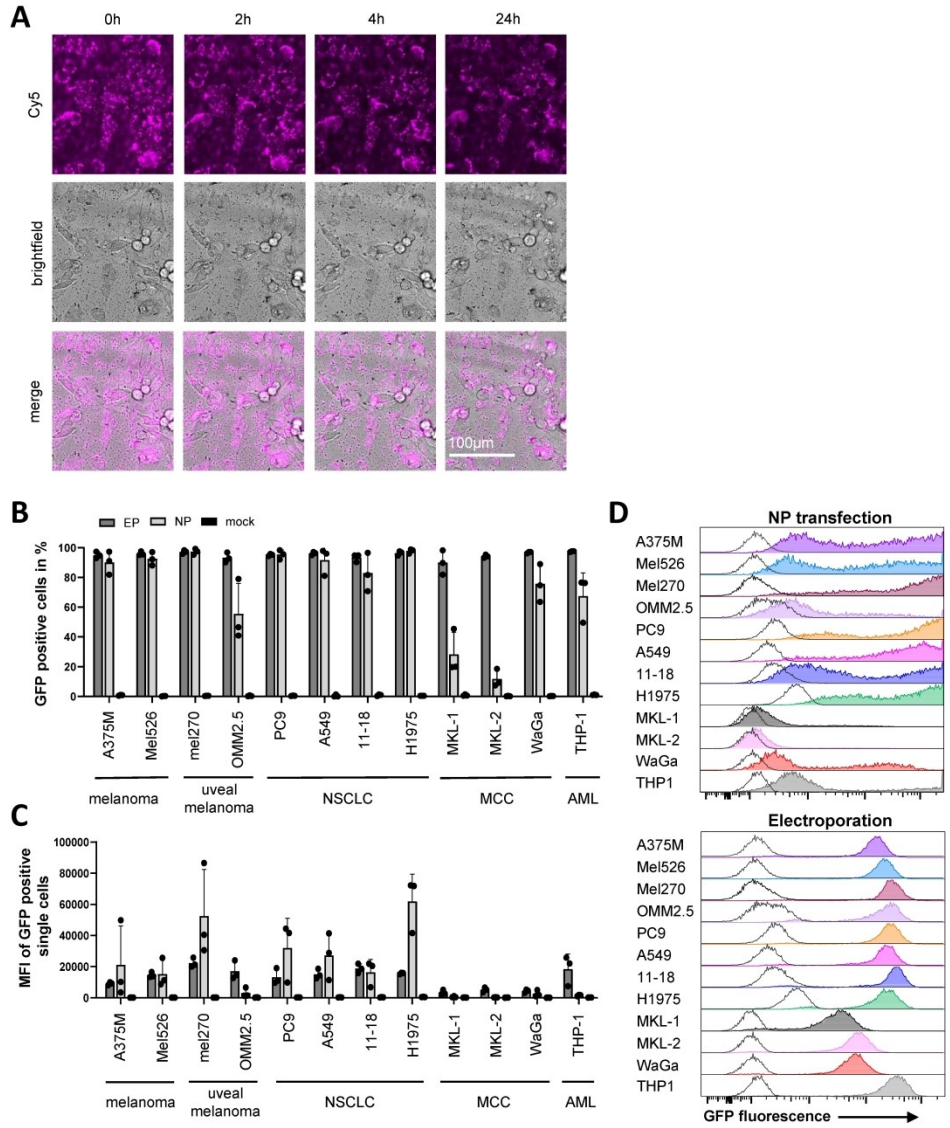

Figure 3: Nanoparticles transfect cell lines of different tumor entities with high efficiency. For the Cy5-labeled nanoparticle (Cy5 NP) transfection assay, Mel526 cells were seeded prior to transfection. Cy5 NPs were then added and imaging was initiated immediately. (A) Representative images from a selected region of interest are shown for the Cy5 fluorescence channel (top), brightfield channel (middle), and the corresponding overlays (bottom) at the indicated time points (0 h, 2 h, 4 h, and 24 h). The tumor cell lines A375M, Mel526, Mel270, OMM2.5, PC9, A549, 11-18, H1975, MKL-1, MKL-2, WaGa, and THP1 were transfected with RNA coding for GFP either by electroporation (EP) or by nanoparticles (NP). The (B) proportion of GFP-positive cells and the (C) mean fluorescence intensity (MFI) was determined by flow cytometry 24 h after transfection. The mean ±SD of 3 independent experiments is depicted. (D) Histograms of GFP expression after transfection with NP and electroporation of the cell lines listed above for one representative experiment. Unstained controls are depicted by the black line and colorless filling.

1135x1412mm (96 x 96 DPI)

View Article Online
DOI: 10.1039/D5NH00667H

View Article Online
DOI: 10.1039/D5NH00667H

Figure 4

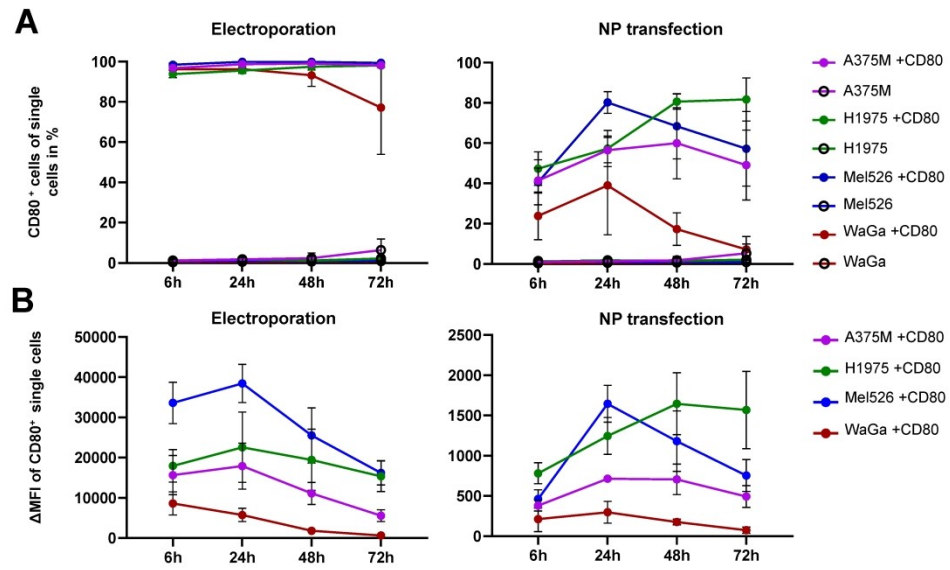

Figure 4: CD80 expression in different tumor cell lines over 72 hours. CD80 mRNA was delivered via electroporation or nanoparticles (NP) transfection to the tumor cell lines A375M (purple), H1975 (green), Mel526 (blue), and WaGa (red). (A) Depicted is the percentage of CD80 positive (CD80+) tumor cells of the referring cell line after 6 h, 24 h, 48 h, and 72 h as mean ±SD conducted in 3 independent experiments. (B) shows the delta mean fluorescence intensity (ΔMFI) of CD80 positive (CD80+) single cells for the experiment (A).

475x325mm (236 x 236 DPI)

View Article Online
DOI: 10.1039/D5NH00667H

Figure 5

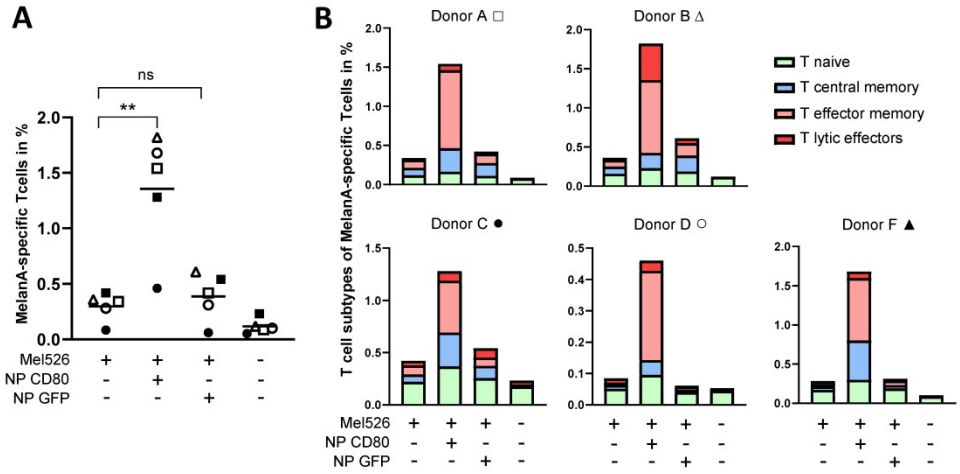

Figure 5: Priming assay with nanoparticle treated tumor cells. Per condition, 106 CD8+ T cells of HLA-A*02:01 donors were co-cultured with 105 Mel526 cells either untreated (-), treated with CD80 RNA-encapsulating nanoparticles (NP CD80) or GFP mRNA-encapsulating nanoparticles (NP GFP). NPs were added at day 0, day 6, day 8, and day 10 to the co-culture. T cells without tumor cells served as control. At day 14 of the co-incubation, the cells were harvested and a MelanA MHC-tetramer staining, as well as an antibody staining for CD8, CCR7, and CD45RA was conducted. (A) Depicted is the percentage of MelanA-specific T cells in the different Mel526 conditions described above for 5 donors. Statistical analysis was performed with a paired t-test, **=p<0.01, ns=not significant. (B) Depicted are the subpopulations of MelanA-specific T cells in relation to the actual percentage of MelanA-specific T cells for each donor separately. T-cell subtypes are divided into naïve T cells (CD45RA/CCR7 double-positive), central memory T cells (CD45RA-, CCR7+), effector memory T cells (CD45RA/CCR7 double-negative) and lytic effector T cells (CD45+, CCR7-).

468x276mm (236 x 236 DPI)

View Article Online
DOI: 10.1039/D5NH00667H

Figure 6

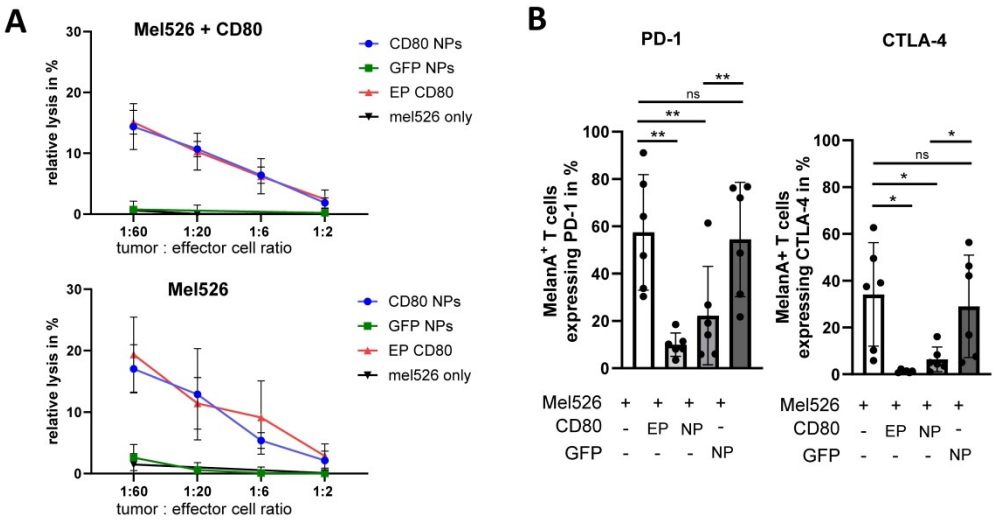

Figure 6: Cytotoxic potential and checkpoint expression of primed T cells. Per condition, 106 CD8+ T cells of HLA-A*02:01 donors were co-cultured with 105 Mel526 cells either untreated (Mel526 only), electroporated with CD80 RNA (EP CD80), treated with CD80 RNA-encapsulating nanoparticles (CD80 NP) or GFP mRNA-encapsulating nanoparticles (GFP NP). NPs were added at day 0, day 6, day 8, and day 10 to the co-culture. T cells without tumor cells served as control. At day 14 of the co-incubation, the cells were harvested and analyzed for their cytotoxic potential and expression of immune checkpoints. (A) In a chromium-based cytotoxicity release assay, the primed T cells (Mel526 only, EP CD80, GFP NP, CD80 NP) as effector cells were incubated with Cr51-labelled Mel526 that were either untreated or electroporated with CD80 RNA at decreasing tumor-to-effector cell ratio of 1:60, 1:20, 1:6 and 1:2. After 4h, the released Cr51 in the supernatant indicated the lysis of the tumor cells. Here, the relative lysis in % is depicted for three individual experiments. (B) The primed T cells were also stained with a MelanA MHC-tetramer staining and antibodies for PD-1 and CTLA-4 to determine the immune checkpoint expression on the antigen-specific T cells. The number of MelanA+ T cells expressing PD-1 or CTLA-4 are displayed for six individual donors. Statistical analysis was performed with a paired t-test, **=p<0.01, *=p<0.05, ns=not significant.

3894x2316mm (38 x 38 DPI)

View Article Online
DOI: 10.1039/D5NH00667H

Figure 7

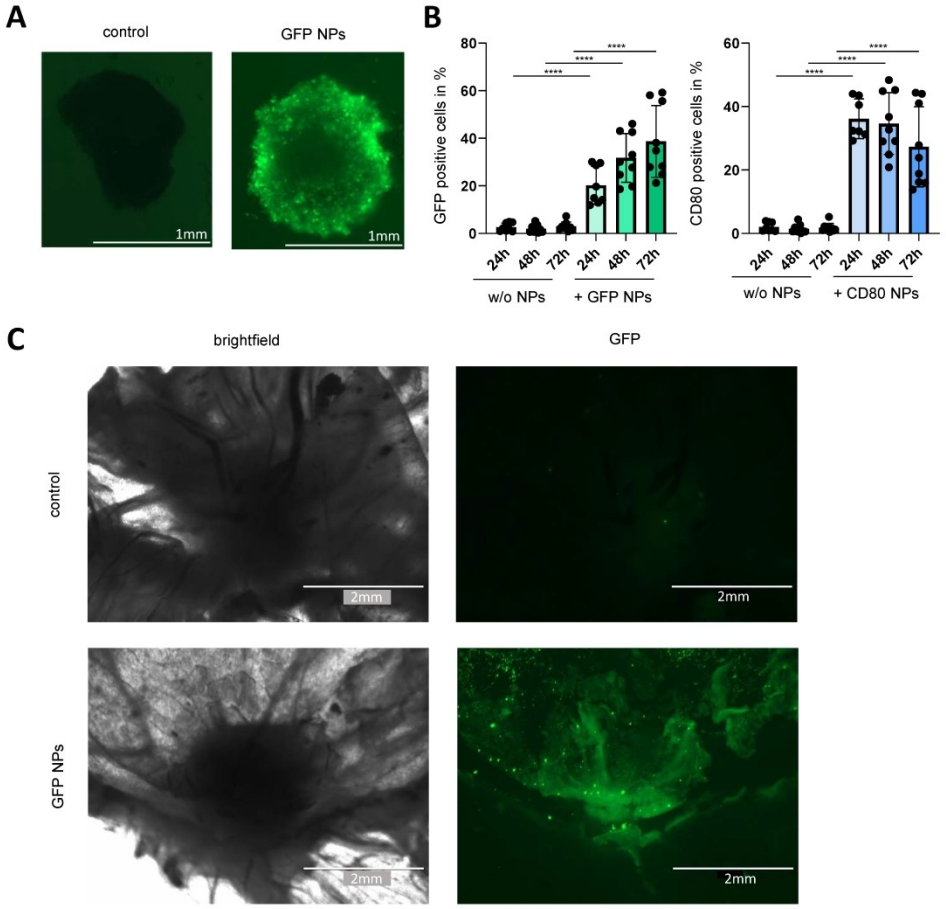

Figure 7. Transfection of Mel526 tumor spheroids in vitro and in ovo. (A) Mel526 tumor spheroids were transfected with GFP nanoparticles (NPs). Images were acquired 24 h post-transfection and non-transfected spheroids served as negative control. (B) Time course of transfection efficiency in Mel526 tumor spheroids treated with GFP mRNA pBAE NPs or CD80 mRNA pBAE NPs for 24, 48, and 72 h. Following treatment with mRNA NPs for the indicated time points, single-cell suspensions were generated by dissociated the spheroids using PBS-EDTA. Cells were subsequently analyzed for CD80 and GFP expression by flow cytometry. Spheroids incubated for similar time periods without NPs served as controls. The experiment was performed three independent times with 2–3 technical replicates each. Statistical analysis was performed with an unpaired t-test, ****=p<0.0001. (C) Mel526 tumor spheroids transplanted onto the CAM and transfected with GFP NPs in ovo. Spheroids were grafted onto the chorioallantoic membrane and allowed to grow for 5 days before nanoparticle treatment; control tumors remained untreated. After 32 h, tumors were excised and imaged immediately by fluorescence microscopy. Top left: untreated tumor spheroid (brightfield). Top right: untreated tumor spheroid (GFP channel). Bottom left: GFP mRNA NP-treated tumor spheroid (brightfield). Bottom right: GFP mRNA NP-treated tumor spheroid (GFP channel).

468x464mm (236 x 236 DPI)

The data supporting this article have been included as part of the Supplementary Information.

View Article Online
DOI: 10.1039/D5NH00667H